Supporting Information

Maltohepatose-Presenting Nanoscale Glycoliposomes for the Delivery of Rifampicin to *E. coli*

Bin Wu, William Ndugire, Xuan Chen, Mingdi Yan*
Department of Chemistry, The University of Massachusetts Lowell, Lowell, MA 01854

*Corresponding Author: Mingdi_Yan@uml.edu

Table of Contents

1. Synthesis of compound 16.

Compound **16** was synthesized following the reaction sequence in **Scheme S1** and previous procedures with modifications.[1,2]

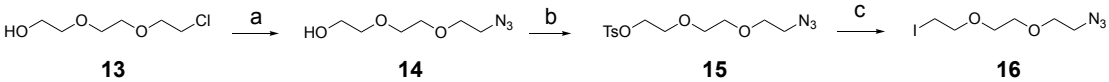

13 **14** **15** **16**

Scheme S1. Synthesis of compound **16**: (a) NaN_3, DMF, 90 °C, overnight (quantitative yield); (b) tosyl chloride (TsCl), triethylamine, 4-dimethylaminopyridine (DMAP), dichloromethane, 0 °C-R.T., 12 h (90%); (c) NaI, DMF, 60 °C, 3 h (85%).

2-(2-(2-Azidoethoxy)ethoxy)ethanol (**14**)

2-(2-(2-Chloroethoxy)ethoxy)ethanol (**13**, 5.0 g, 30 mmol) and sodium azide (3.9 g, 60 mmol) were added to DMF (40 mL). The mixture was stirred at 90 °C under Ar atmosphere overnight. The solvent was evaporated under reduced pressure at 50 °C, and water was added. The solution was then extracted with ethyl acetate for three times. The organic phase was combined, washed with brine, and dried over Na_2SO_4. After evaporation of the solvent, the crude product was purified by flash column chromatography (hexanes/ethyl acetate 1:1 v/v), giving compound **14** as a colorless oil (5.2 g, quant.) ^{1}H NMR (500 MHz, $CDCl_3$) δ 3.78 – 3.72 (m, 2H), 3.72 – 3.67 (m, 2H), 3.65 – 3.59 (m, 2H), 3.46 – 3.37 (m, 2H).

2-(2-(2-Azidoethoxy)ethoxy)ethyl 4-methylbenzenesulfonate (**15**)

In a solution of compound **14** (4.3 g, 24.5 mmol) in dry DCM (50 mL), triethylamine (4.1 mL, 29.4 mmol), DMAP (295 mg, 2.4 mmol) and 4 Å molecular sieves were added. The mixture was stirred at room temperature for 20 mins and then cooled down to 0 °C. A solution of tosyl chloride (5.6 g, 29.4 mmol) in dry DCM (20 mL) was added. After the reaction mixture was warmed up to room temperature, it was stirred overnight. The mixture was poured into 1 M HCl, extracted by DCM three times. The organic phase was combined, washed with $NaHCO_3$ solution, brine, dried over Na_2SO_4, and the solvent was evaporated. The crude product was purified by flash column chromatography (hexanes/ethyl acetate, 3:2 v/v), giving compound **15** as a colorless oil (7.26 g, 90%). ^{1}H NMR (500 MHz, $CDCl_3$) δ 7.83 – 7.78 (m, 2H), 7.39 – 7.32 (m, 2H), 4.19 – 4.15 (m, 2H), 3.72 – 3.69 (m, 2H), 3.64 (t, J = 5.4 Hz, 2H), 3.61 (s, 4H), 3.39 – 3.33 (m, 2H), 2.45 (s, 3H).

Azido-2-(2-(2-iodoethoxy)ethoxy)ethane (**16**)

Compound **15** (3.3 g, 10.0 mmol) and potassium iodide (4.98 g, 30.0 mmol) were added to DMF (50 mL). The mixture was stirred at 50 °C under Ar atmosphere for 5 hours. After the solvent was evaporated under reduced pressure, the residue was washed with water and extracted with ethyl acetate three times. The organic phase was combined, washed with brine, and dried over Na_2SO_4. After evaporation of the

solvent, the crude product was purified by flash column chromatography (hexanes/ethyl acetate 2:1 v/v), giving compound **16** (2.43 g, 85%) as a colorless oil. ^{1}H NMR (500 MHz, $CDCl_3$): δ 3.77 (t, 2 H, J = 6.6 Hz), 3.70 (t, 2H, J = 5.1 Hz), 3.68 (s, 4 H,), 3.40 (t, 2 H, J = 5.1 Hz), 3.27 (t, 2 H, J = 6.6 Hz).

2. Synthesis of compound 17

Compound **17** was synthesized as shown in **Scheme S2** following a reported procedure.[3]

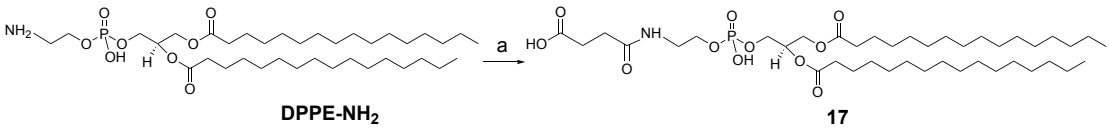

Scheme S2. Synthesis of compound **17**: (a) succinic anhydride, triethylamine, R.T., 4 h (83%).

DPPE-NH_2 (300 mg, 0.425 mmol) and Et_3N (150 μL) were dissolved in 25 mL of $CHCl_3$/MeOH (9:1). Succinic anhydride (60 mg, 0.6 mmol) was added, and the solution was stirred at room temperature for 5 h. The reaction mixture was acidified by adding 50 mL of $CHCl_3$ and then 50 mL of 0.02 M citrate/0.02 M phosphate buffer (pH 5.5), and the mixture was stirred for 30 min. The aqueous phase was extracted three times with 60 mL of $CHCl_3$, and the combined organic phases were dried over anhydrous sodium sulfate, and solvent was removed in vacuo to give the product **17** as a viscous solid (315 mg, 83%). ^{1}H NMR (500 MHz, $CDCl_3$) δ 7.51 (t, J = 4.8 Hz, 1H, NHCO), 5.23 (dt, J = 9.0, 4.4 Hz, 1H, CH_2CHCH_2), 4.38 (dd, J = 12.0, 3.4 Hz, 1H, CH_2CHCH_2OP), 4.16 (dd, J = 12.0, 6.6 Hz, 1H), 4.08 – 3.92 (m, 4H, CH_2CHCH_2OP and $POCH_2CH_2NH$), 3.47 (q, J = 4.8 Hz, 2H, $PCOCH_2CH_2NH$), 3.04 (q, J = 7.3 Hz, 6H, $(CH_3CH_2)_3N$), 2.67-2.53 (m, 4H, $NHCOCH_2CH_2COO$), 2.29 (q, J = 7.2 Hz, 4H, $2\times CH_3(CH_2)_{12}CH_2CH_2CO$), 1.67 – 1.53 (m, 4H, $2\times CH_3(CH_2)_{12}CH_2CH_2CO$), 1.36 – 1.22 (m, 57H, $2\times CH_3(CH_2)_{12}CH_2$, $(CH_3CH_2)_3N$), 0.88 (t, J = 6.9 Hz, 6H, $2\times CH_3(CH_2)_{12}CH_2$).

3. Standard calibration curve of rifampicin

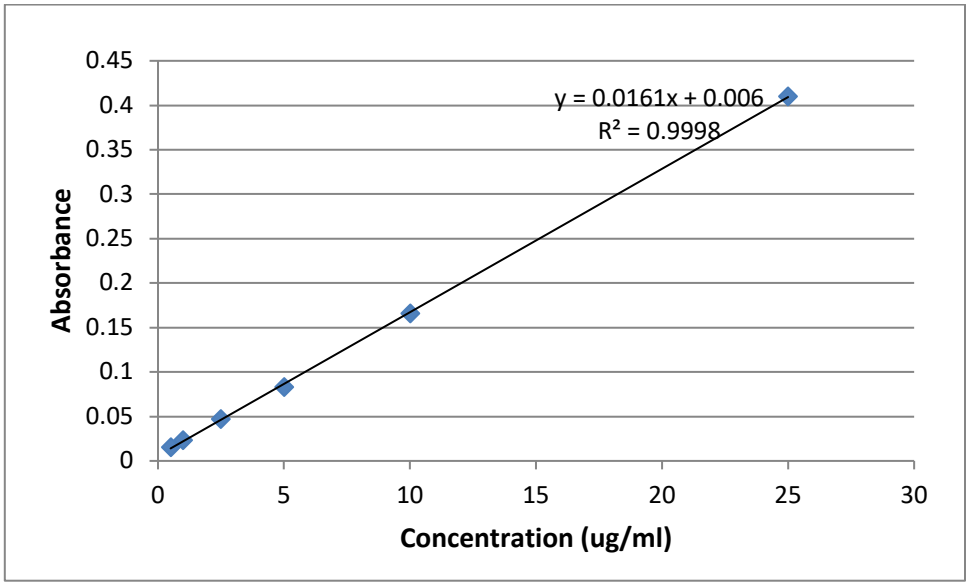

Figure S1. Standard calibration curve of rifampicin, constructed by measuring the absorbances of varying concentrations of rifampicin solutions in DMSO at 475 nm.

4. Calculation of apparent first-order release constant k_{obs} and permeability coefficient P_{app} for rifampicin release from liposomes.

The model reported by Anderson and coworkers was used.[4] The following equation describes the concentration of drug inside the liposomes vs. dialysis time:

$$-\frac{dC_i^t}{dt} = k_{obs}(C_i^t - C_o^t) \qquad \text{(S1)}$$

where C_i^t and C_o^t are the drug concentrations inside and outside the liposomes at time t, respectively, and k_{obs} is the first-order rate constant.

Since the total mass of the drug in the sample is a constant, and C_i^t is equal to C_o^t at equilibrium, the following equation is derived:

$$C_o^t = \frac{1}{V_0}[(V_i + V_0)C_0^\infty - V_i C_i^t] \qquad \text{(S2)}$$

where V_i and V_0 are the volumes of the aqueous solutions inside and outside the liposomes, respectively.

Considering that $V_i << V_0$, Eq. 1 becomes

$$\frac{dC_0^t}{dt} = k_{obs}(C_0^\infty - C_0^t) \qquad \text{(S3)}$$

which can be solved to give

$$In[(C_0^{\infty} - C_0^0)/(C_0^{\infty} - C_0^t)] = k_{obs}t \qquad \text{(S4)}$$

The apparent permeability coefficient P_{app} can be obtained from the following equation:

$$P_{app} = k_{obs}V/A \qquad \text{(S5)}$$

where V is the entrapped volume and A is the surface area of the liposomes. The V/A ratio can be obtained from the following: V/A = d/6, where d is the hydrodynamic diameter of the liposome.

5. Standard calibration curves of Man-DPPE and G7-DPPE

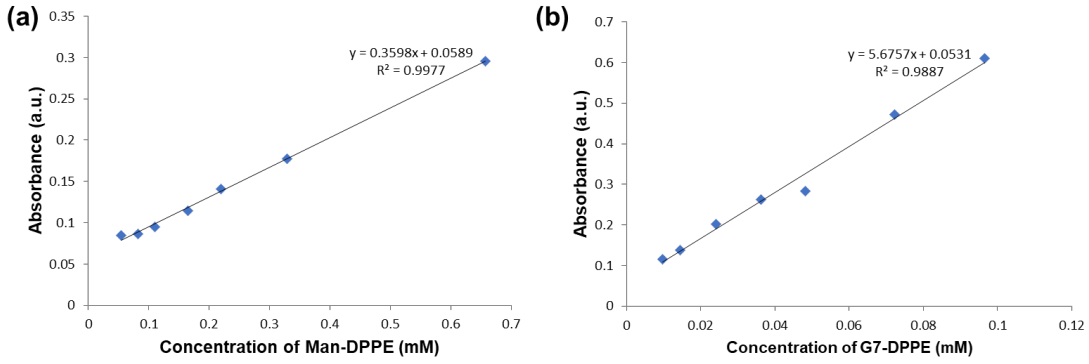

Figure S2. Calibration curves for (a) Man-DPPE, and (b) G7-DPPE. Solutions of varying concentrations of G7-DPPE or Man-DPPE were treated with anthrone solution (0.5 wt% in 98% sulfuric acid) following the procedure described in the Experimental section of the manuscript. The absorbance at 620 nm of the resulting solution was measured, and the data were plotted against the concentration of the glycolipid.

6. FRET

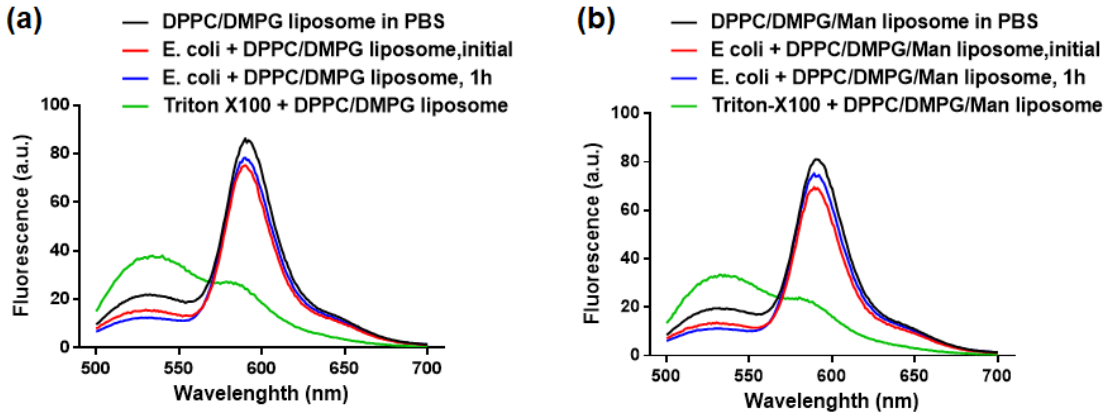

Figure S3. Bacterium-liposome interactions by FRET for NBD/Rh-labeled fluid (a) liposomes, and (b) Man-glycoliposomes: fluorescence spectra of liposomes alone (black), liposomes after mixing with Triton X-100 (green) or *E. coli* immediately (red) and after 1 h incubation (blue). Excitation: 460 nm.

Table S1. Fluorescence intensity at 590 nm (Rh) and 536 nm (NBD) of NBD/Rh-labeled glycoliposomes before and after incubations with *E. coli* ORN208.

Sample	Fluorescence intensity at 590 nm (a.u.)			Fluorescence intensity at 536 nm (a.u.)			$I_{590\ nm}/I_{536\ nm}$		
	G7-	Man-	liposome	G7-	Man-	liposome	G7-	Man-	liposome
NBD/Rh-labeled fluid liposomes	64.9	81.2	86.2	25.7	19.5	21.7	2.5	4.2	4.0
Addition of Triton X-100	23.4	21.0	24.3	36.2	32.8	37.3	0.6	0.6	0.7
Addition of bacteria, immediate	54.8	68.7	75.3	16.8	13.2	15.1	3.3 (32%)	5.2 (23%)	5.0 (25%)
Addition of bacteria, after 1 h incubation	62.9	73.9	78.3	14.6	11.1	12.2	4.3 (72%)	6.7 (60%)	6.4 (60%)

7. Confocal fluorescence microscopy

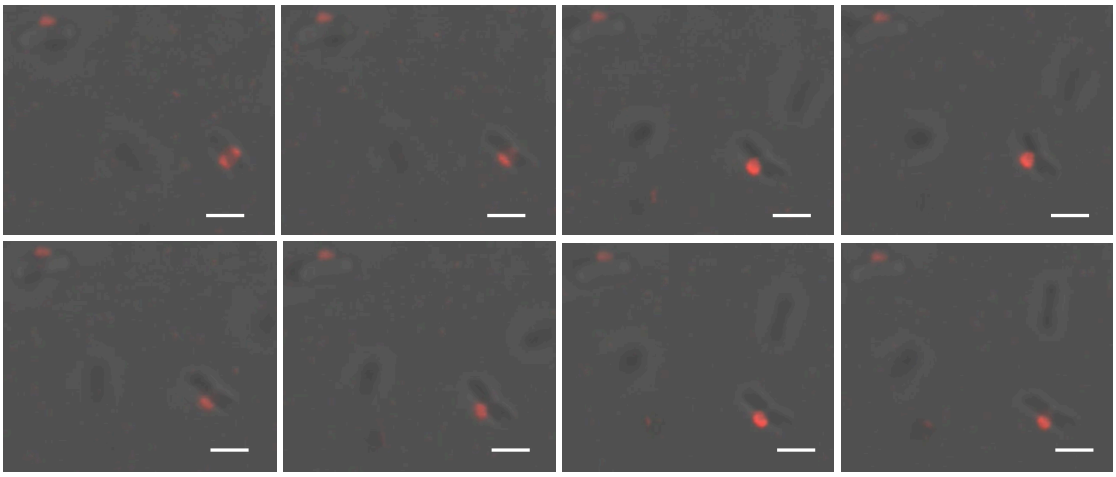

Figure S4. Confocal fluorescence images of NBD/Rh-labeled fluid G7-glycoliposomes incubated with *E. coli* ORN208 during a course of 5 min. Scale bars: 2 μm.

8. ^{1}H NMR, ^{13}C NMR, and ^{31}P NMR spectra

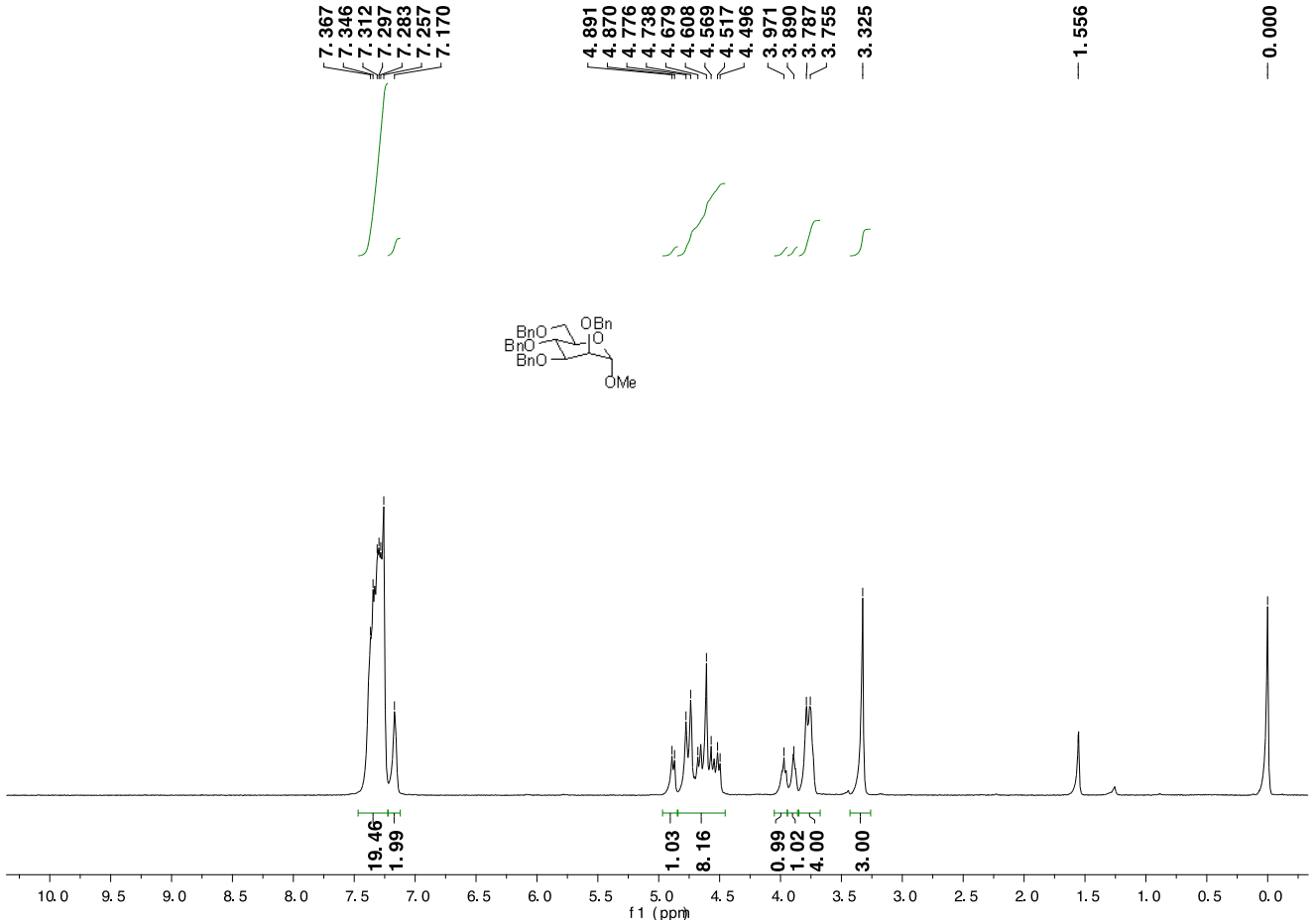

Figure S5. ^{1}H NMR spectrum of methyl 2,3,4,6-tetra-*O*-benzyl-α-D-mannopyranoside **(1)** in $CDCl_3$.

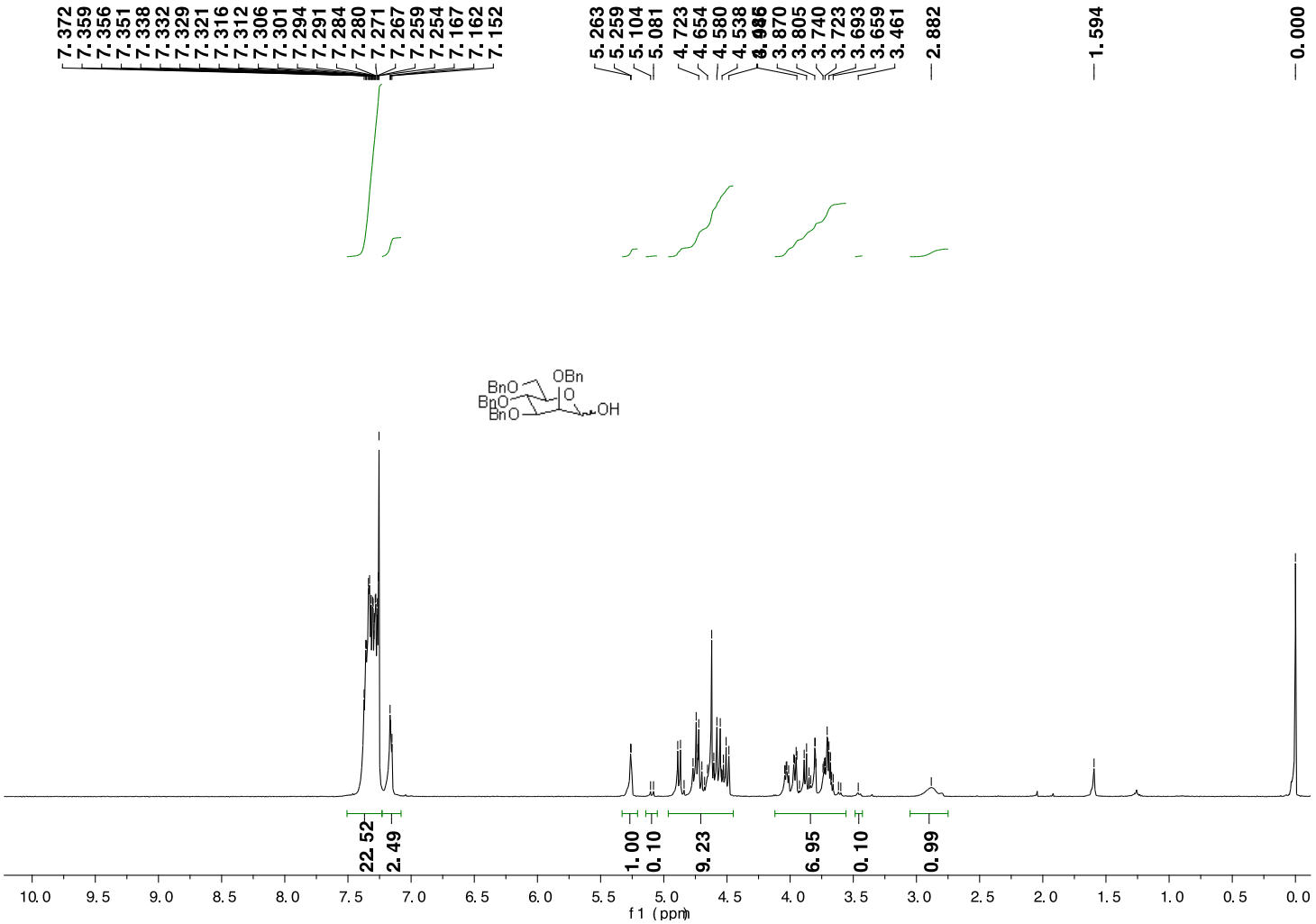

Figure S6. ^{1}H NMR spectrum of 2,3,4,6-tetra-*O*-benzyl-α/β-D-mannopyranose **(2)** in $CDCl_3$.

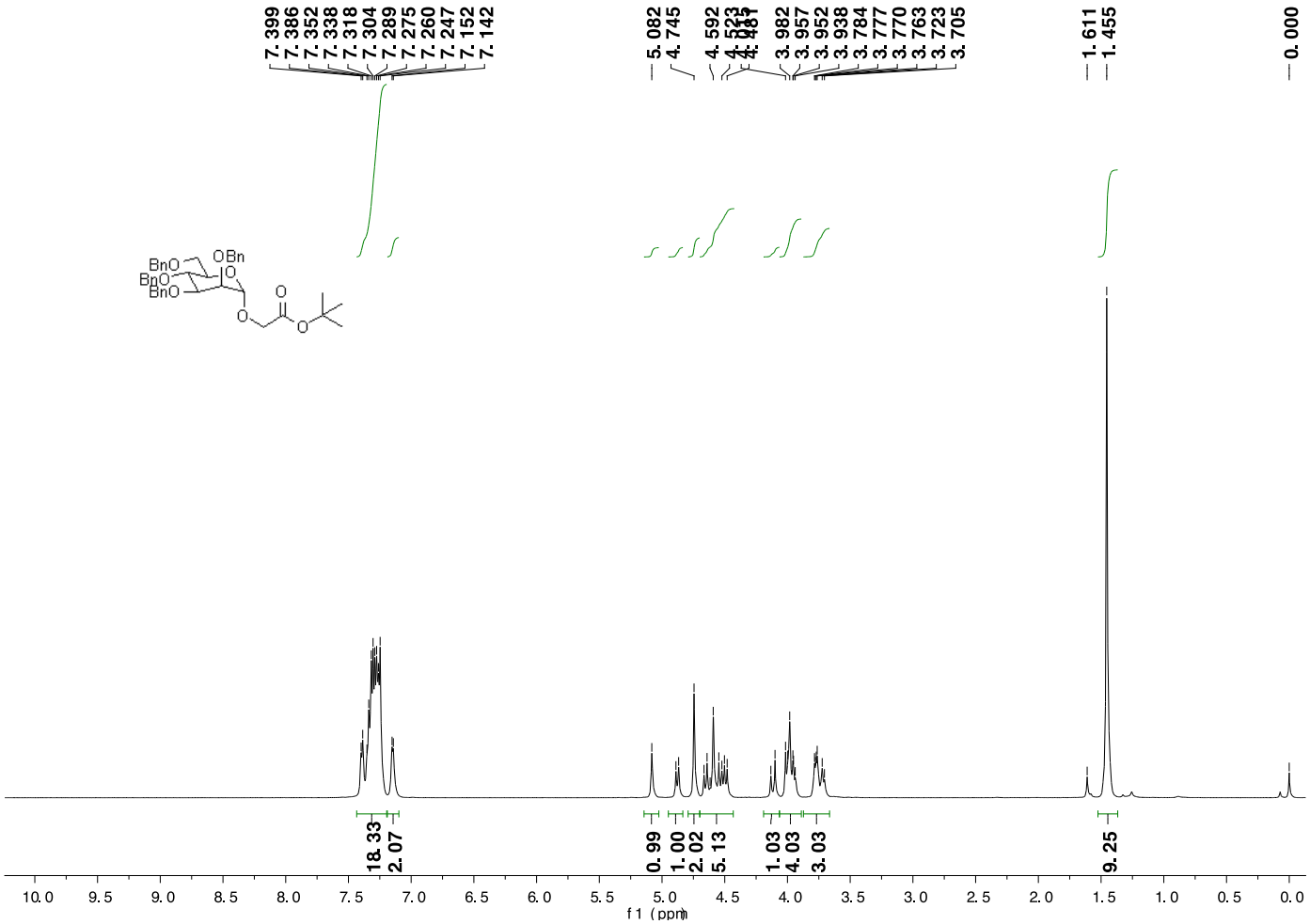

Figure S7. ^{1}H NMR spectrum of (*t*-butyloxycarbonyl) methyl 2,3,4,6-tetra-*O*-benzyl-α-D-mannopyranoside **(3)** in $CDCl_3$.

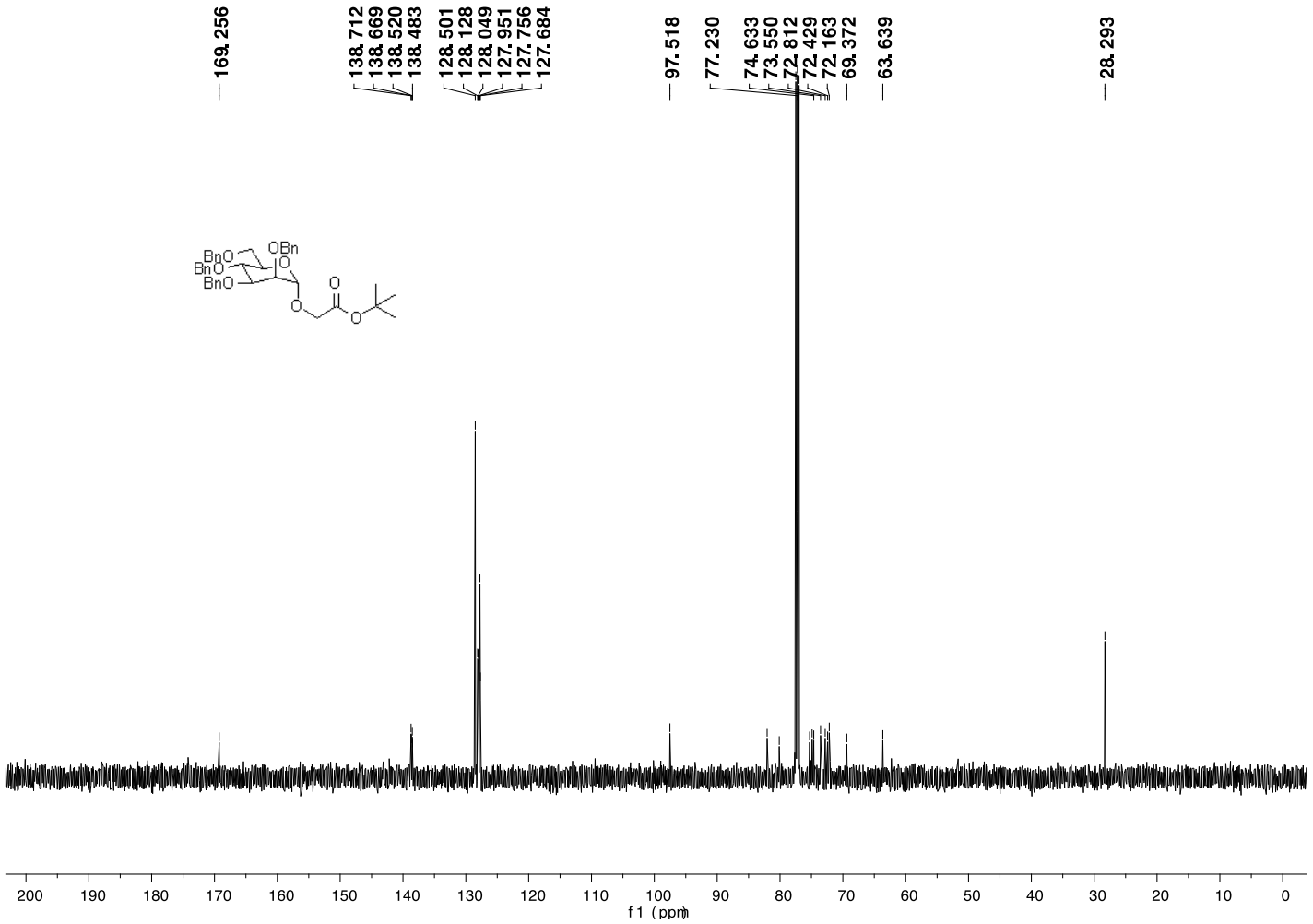

Figure S8. ^{13}C NMR spectrum of (*t*-butyloxycarbonyl) methyl 2,3,4,6-tetra-*O*-benzyl-α-D-mannopyranoside **(3)** in $CDCl_3$.

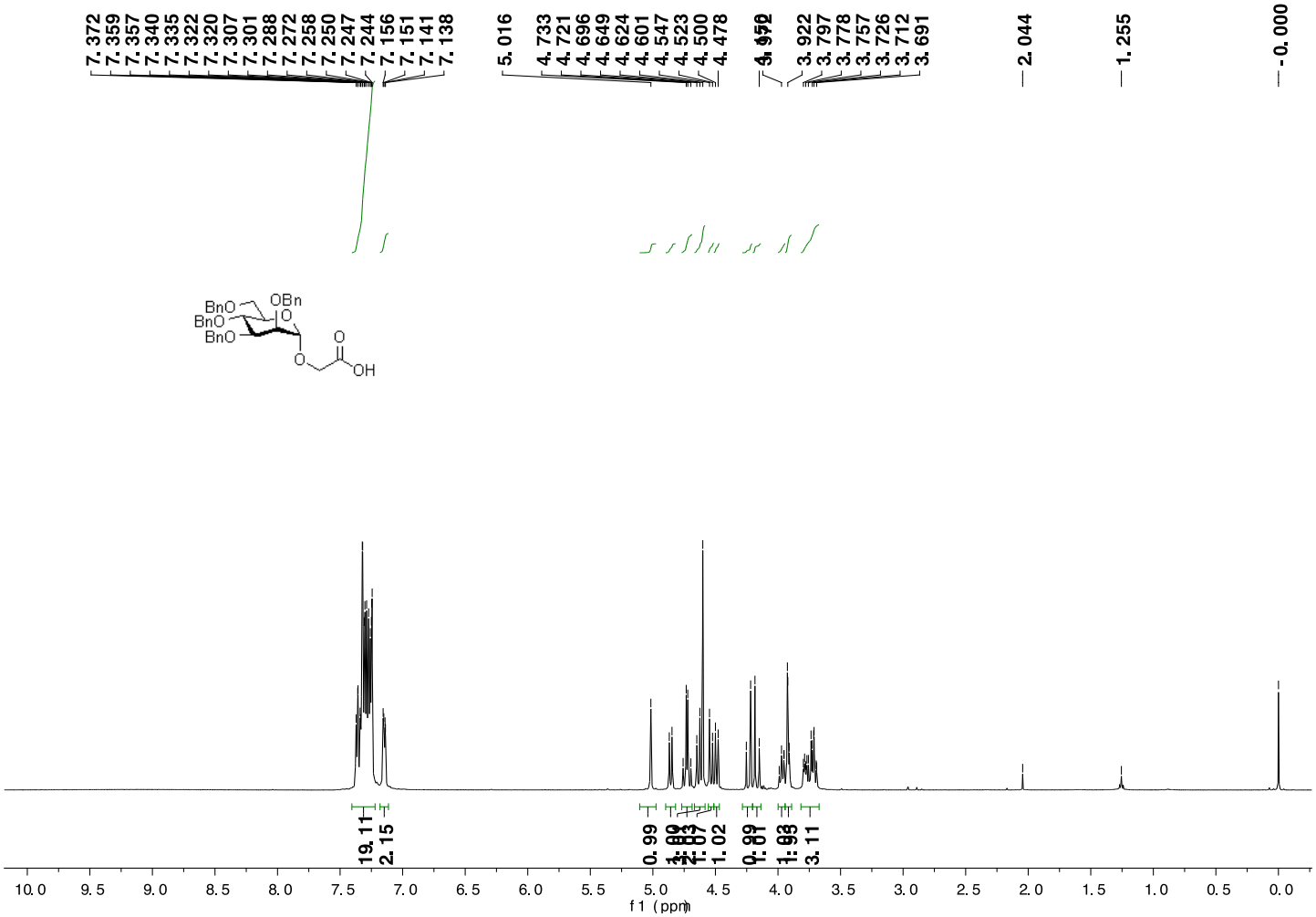

Figure S9. ^{1}H NMR spectrum of **4** in $CDCl_3$.

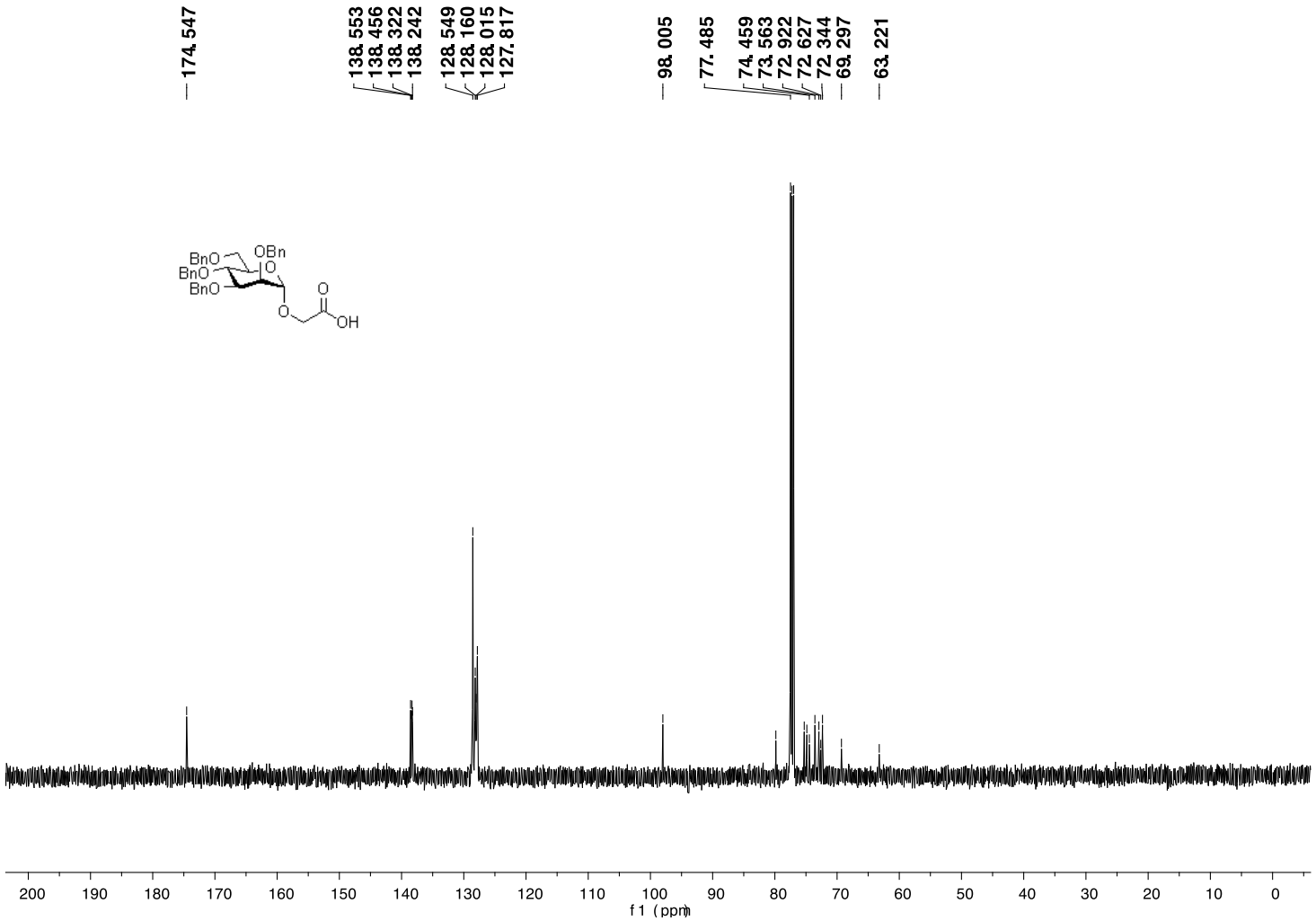

Figure S10. ^{13}C NMR spectrum of **4** in $CDCl_3$.

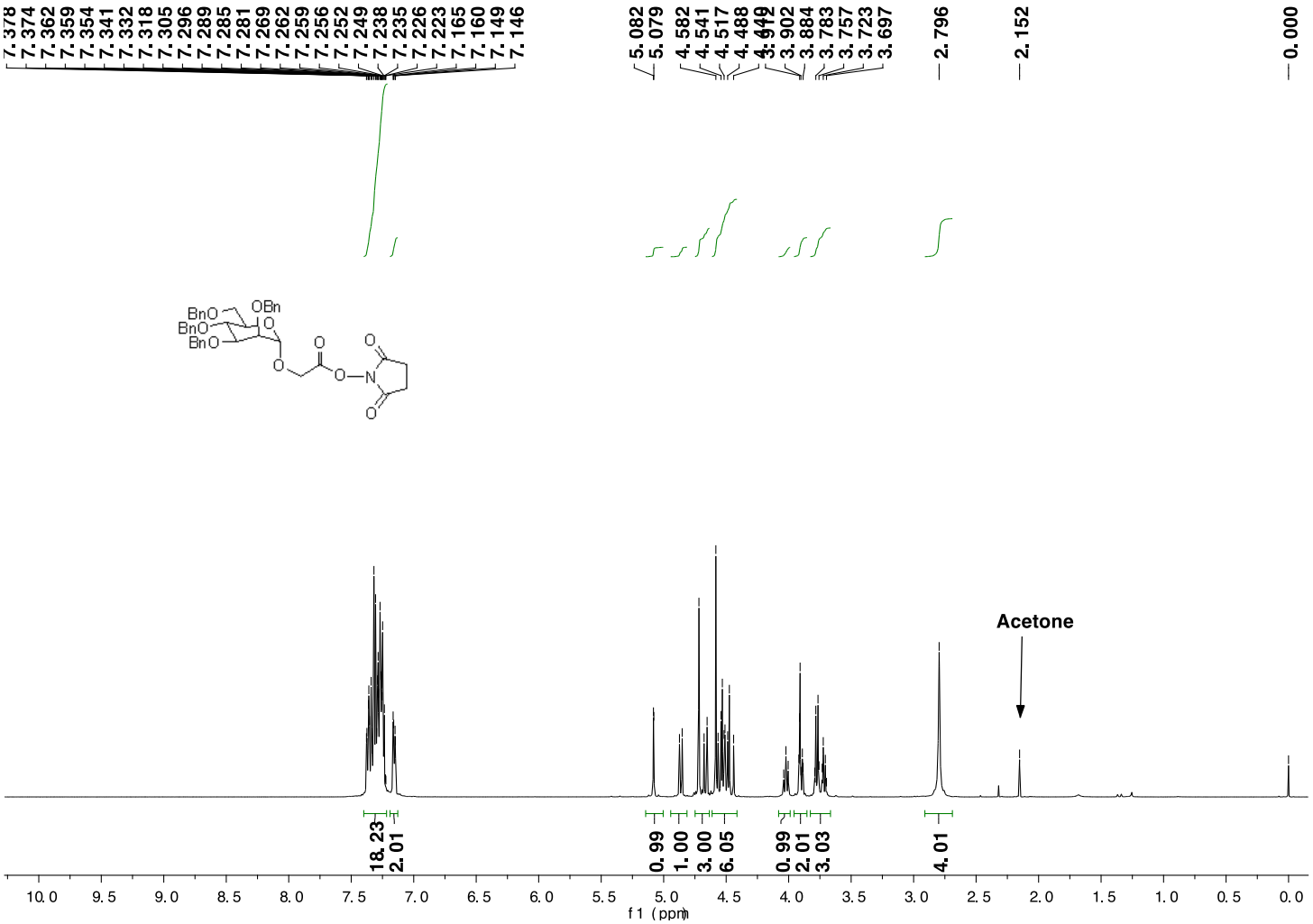

Figure S11. ^{1}H NMR spectrum of **5** in $CDCl_3$.

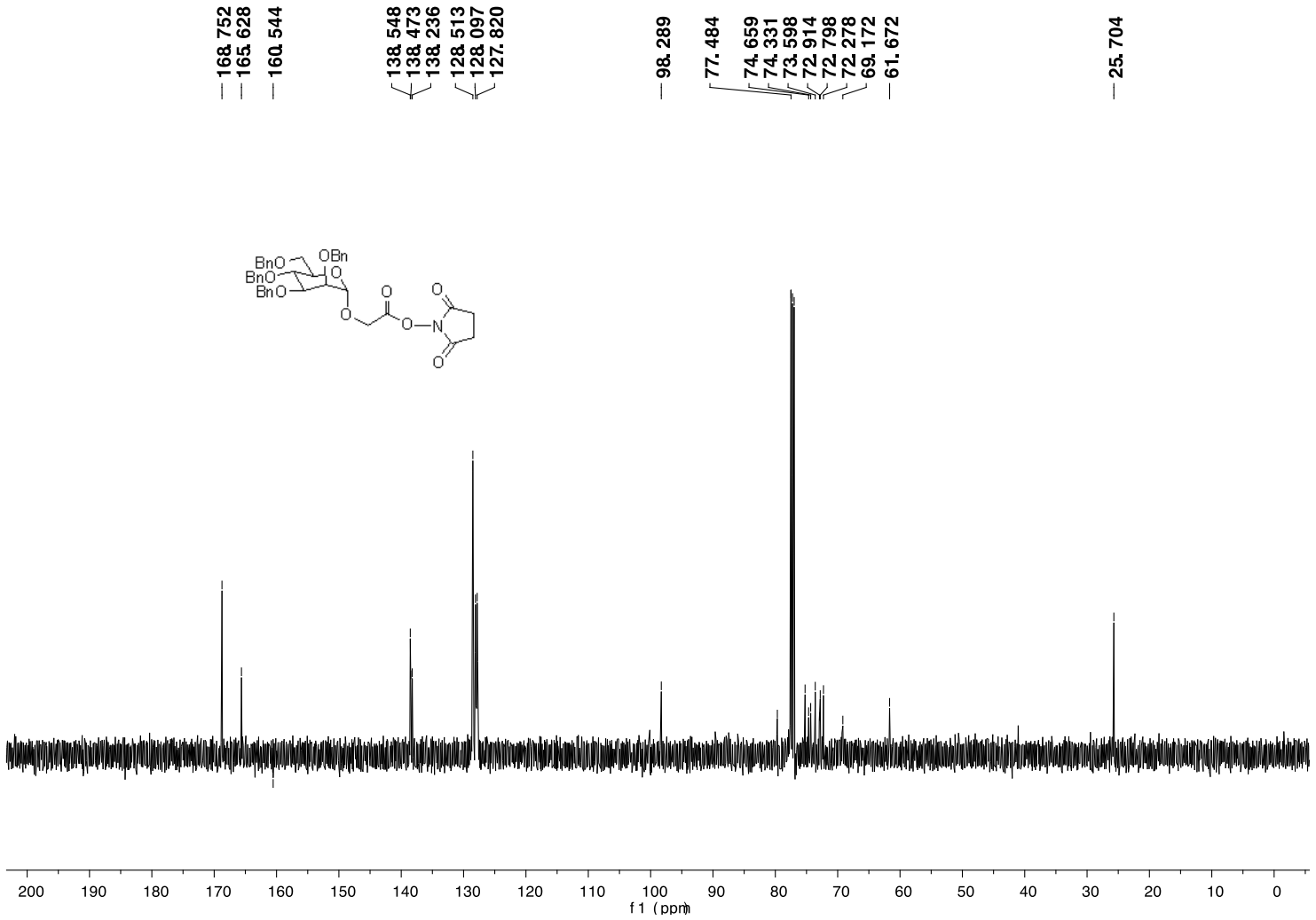

Figure S12. ^{13}C NMR spectrum of **5** in $CDCl_3$.

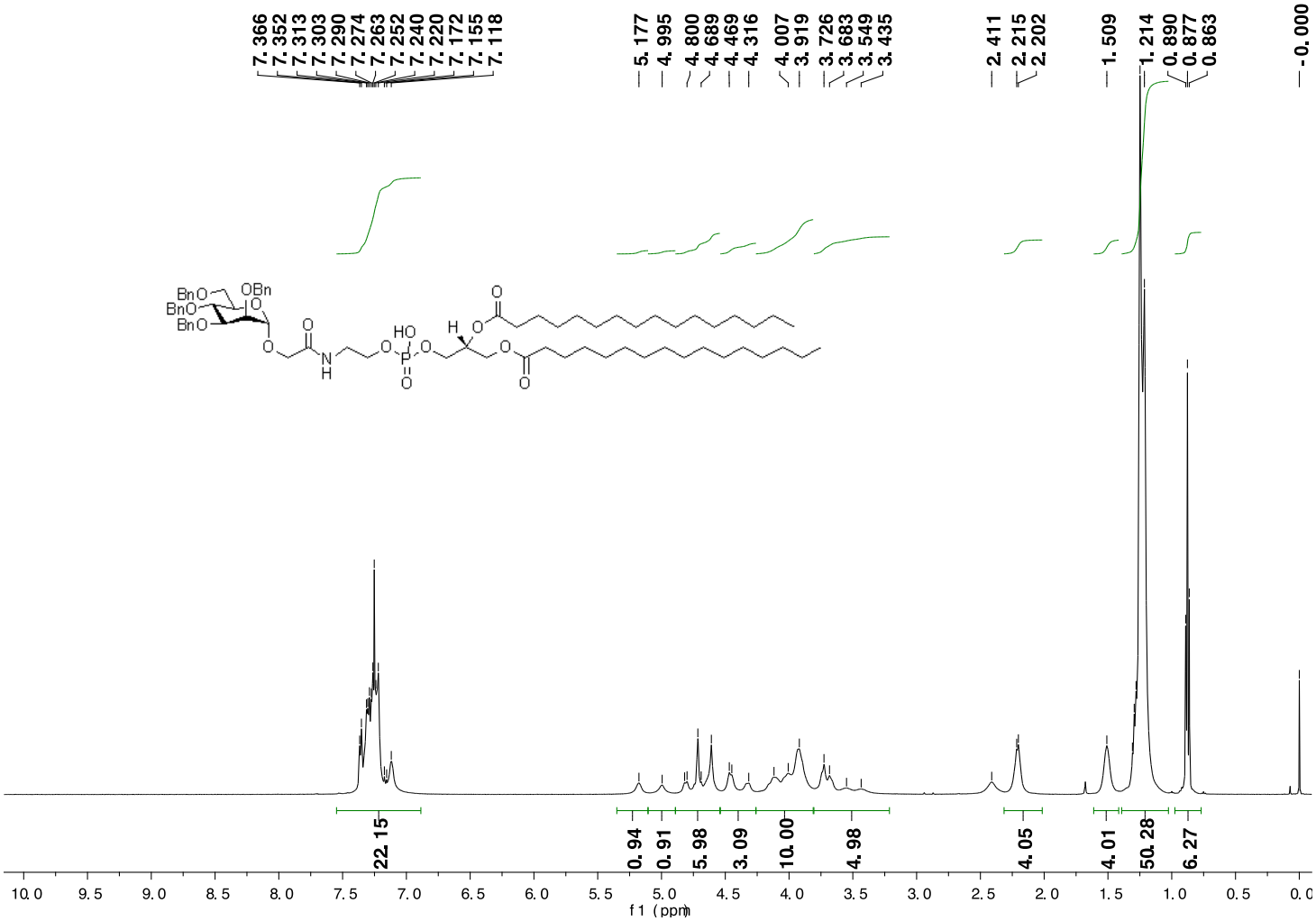

Figure S13. ^{1}H NMR spectrum of **6** in $CDCl_3$.

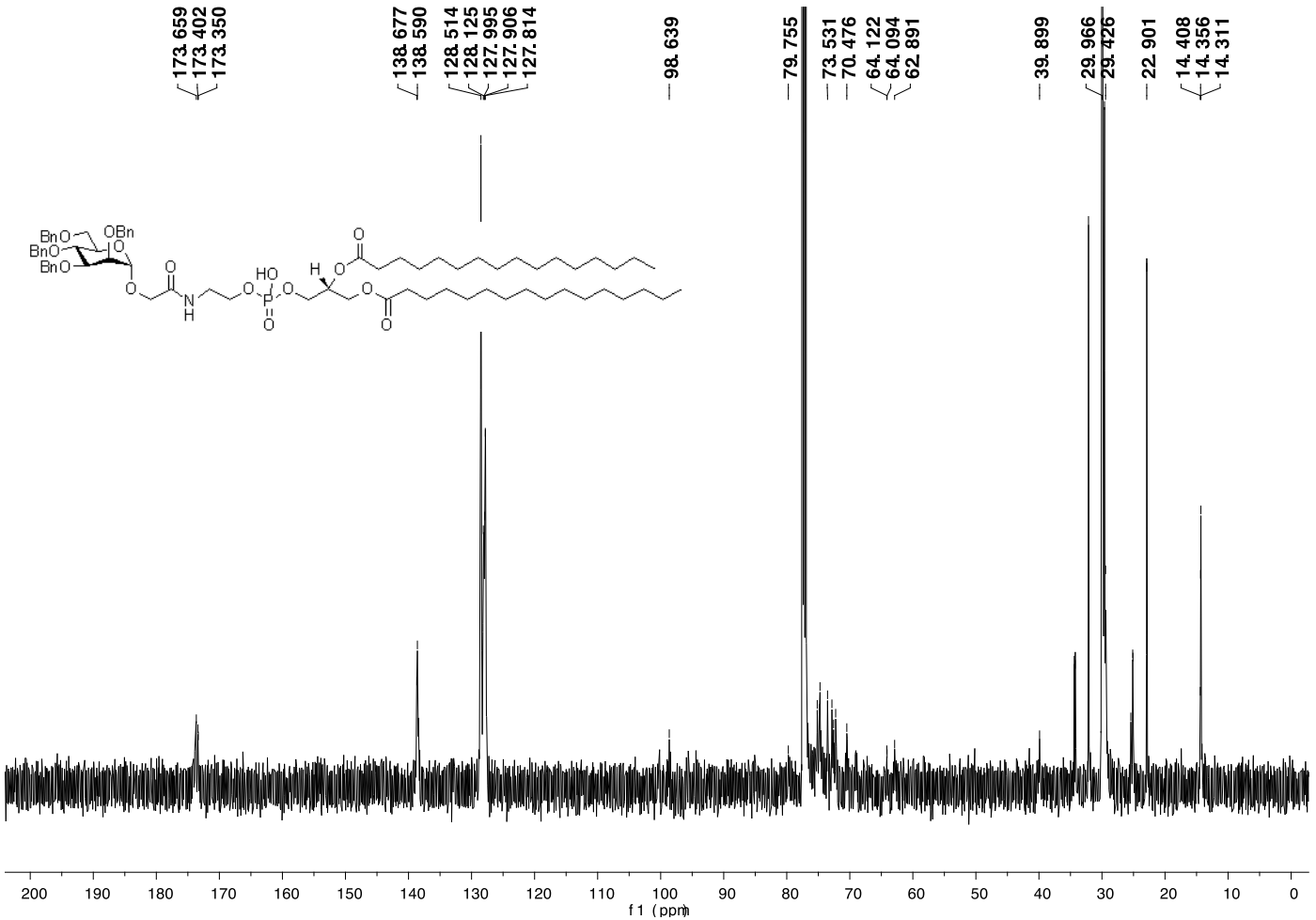

Figure S14. ^{13}C NMR spectrum of **6** in $CDCl_3$.

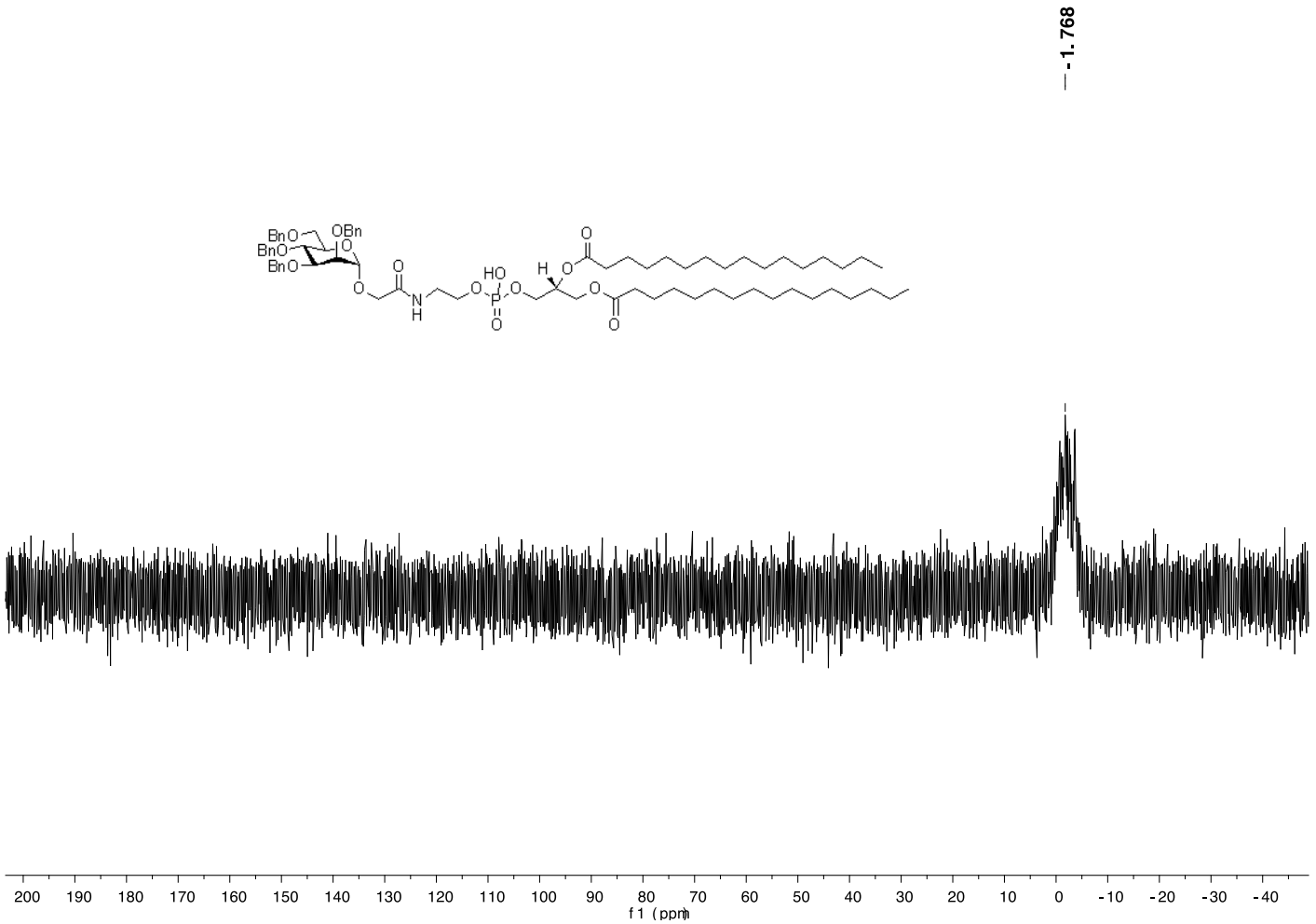

Figure S15. ^{31}P NMR spectrum of **6** in $CDCl_3$.

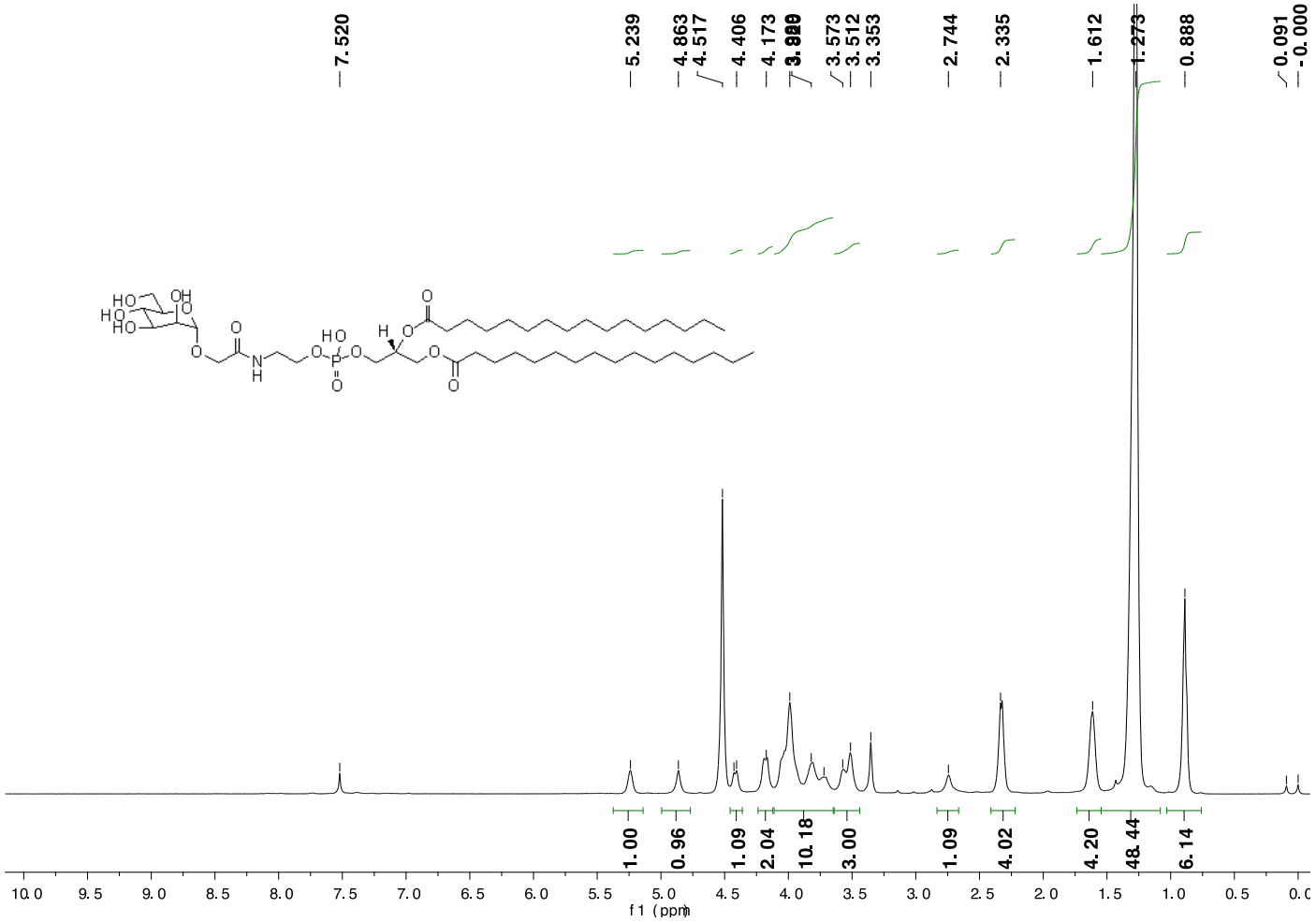

Figure S16. ^{1}H NMR spectrum of **Man-DPPE** in $CDCl_3/CD_3OD/D_2O$ (7:4:0.1 v/v/v).

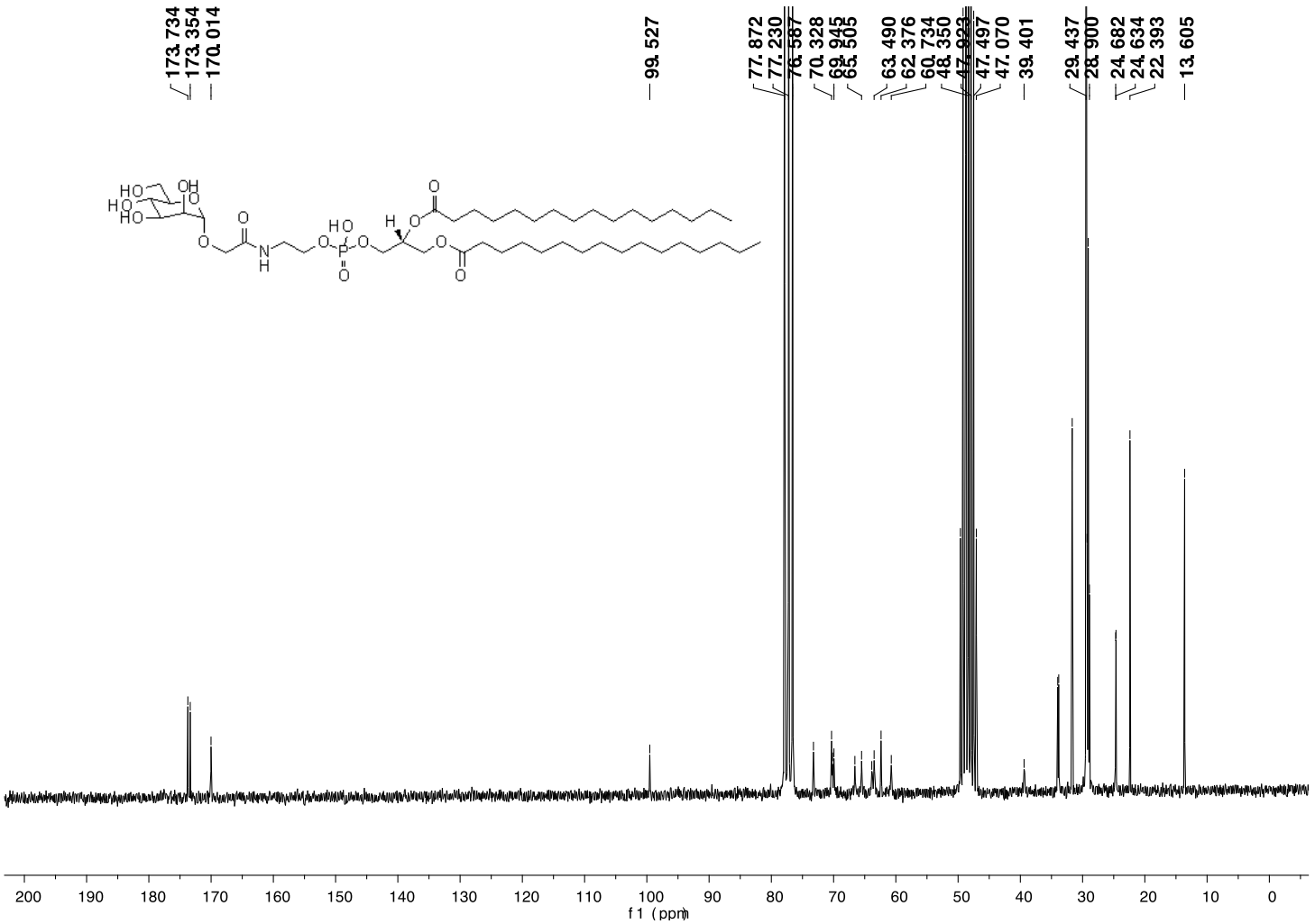

Figure S17. ^{13}C NMR spectrum of **Man-DPPE** in $CDCl_3/CD_3OD/D_2O$ (7:4:0.1 v/v/v).

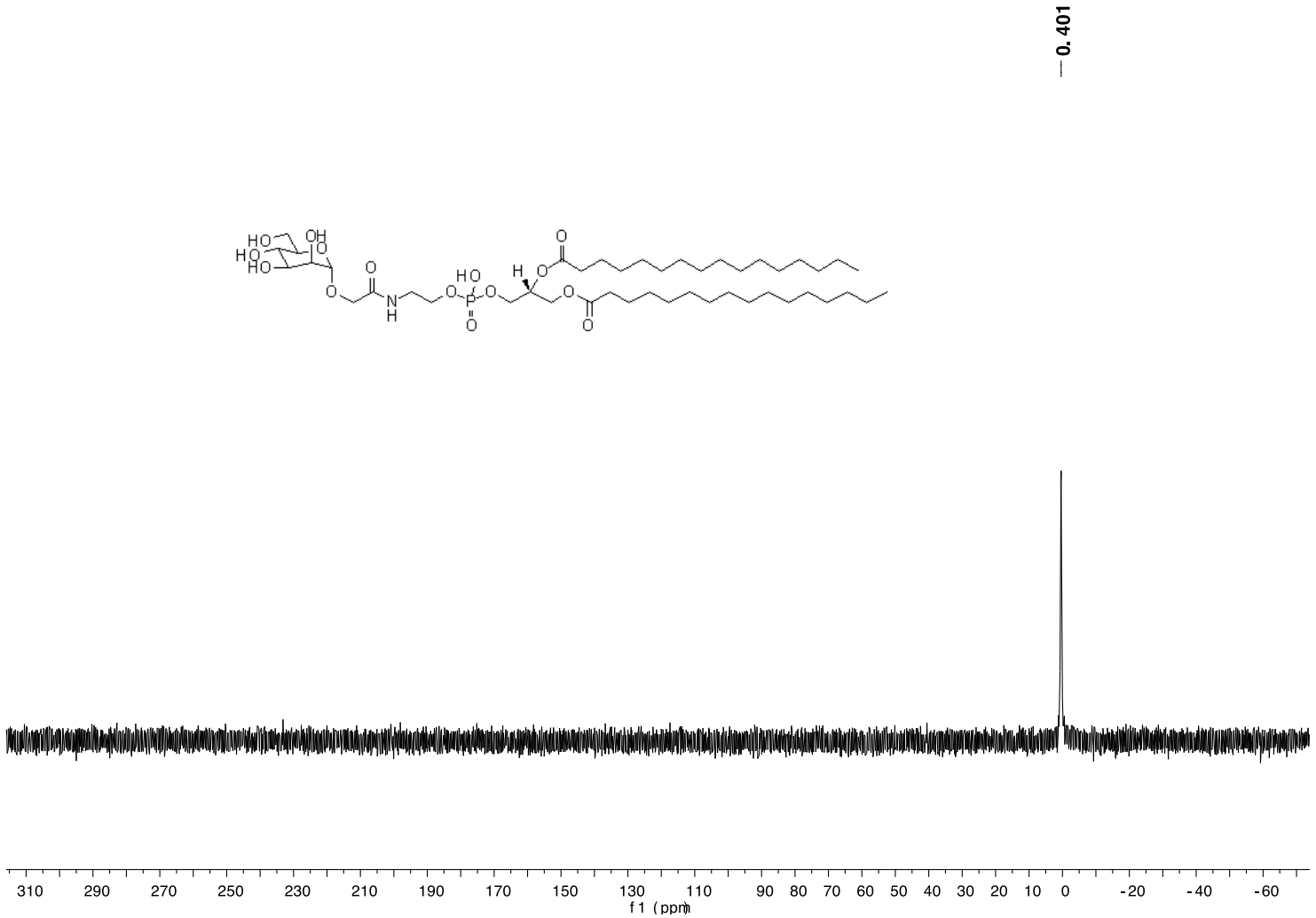

Figure S18. ^{31}P NMR spectrum of **Man-DPPE** in $CDCl_3/CD_3OD/D_2O$ (7:4:0.1 v/v/v).

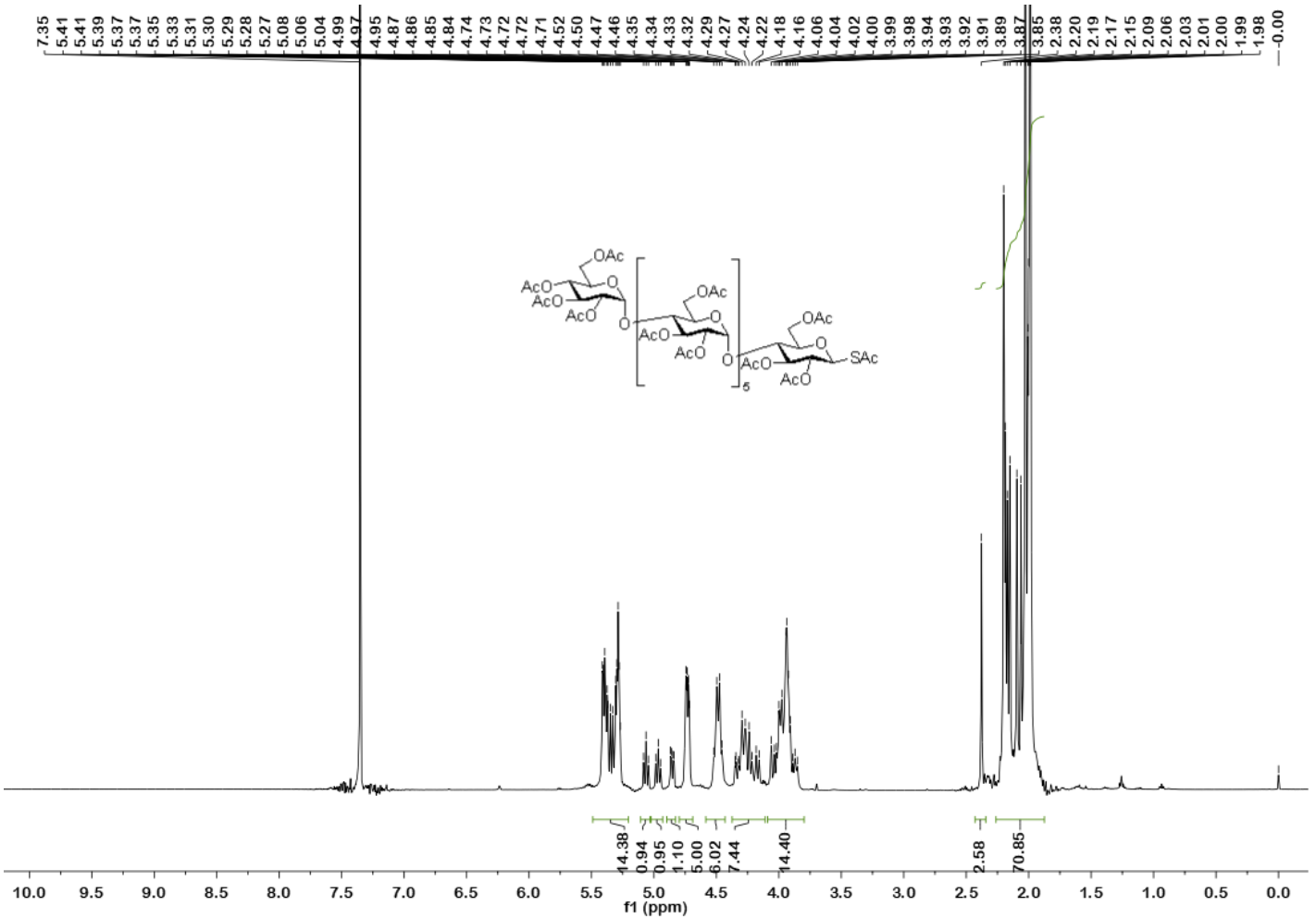

Figure S19. ^{1}H NMR spectrum of **9** in $CDCl_3$

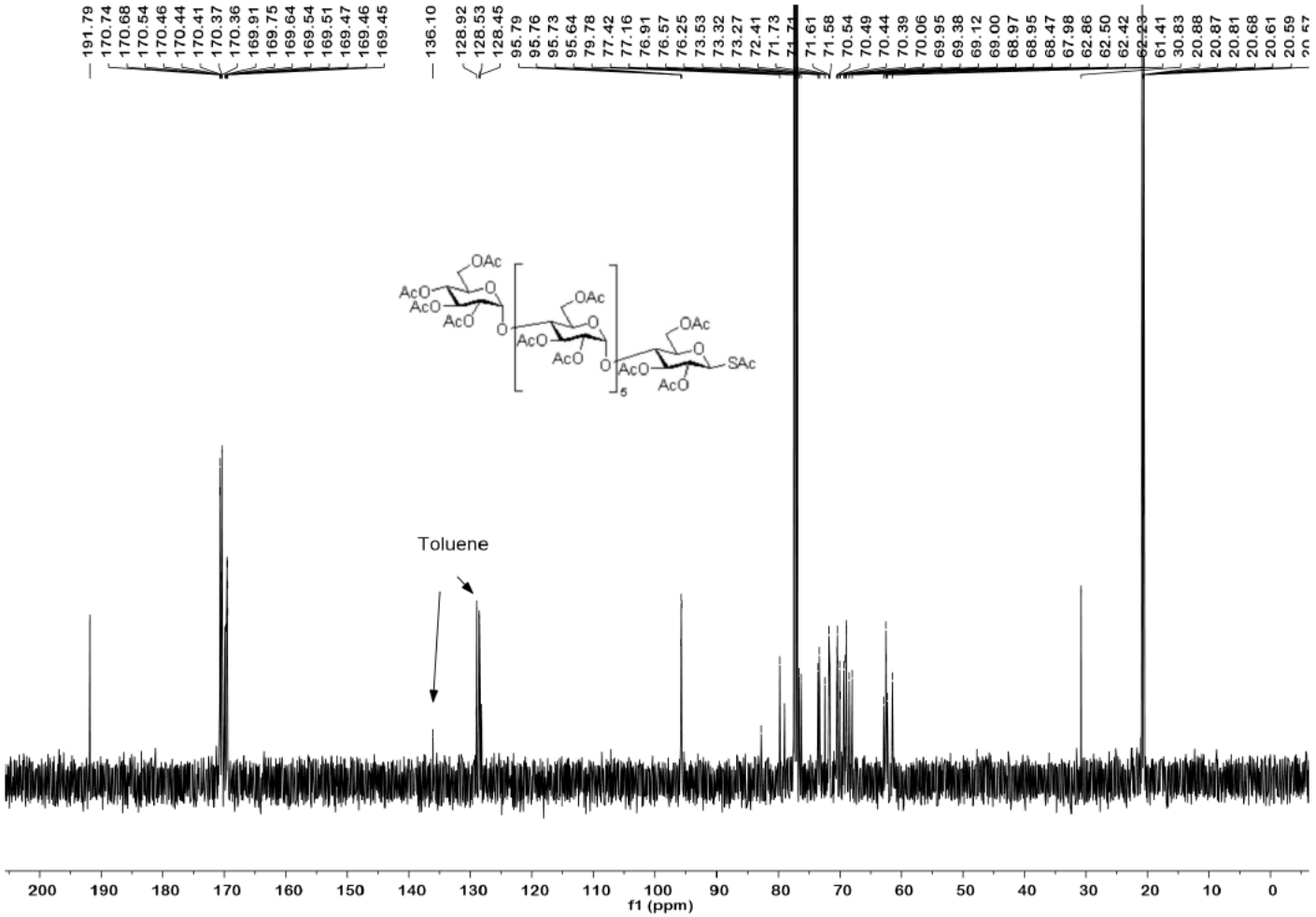

Figure S20. ^{13}C NMR spectrum of **9** in $CDCl_3$.

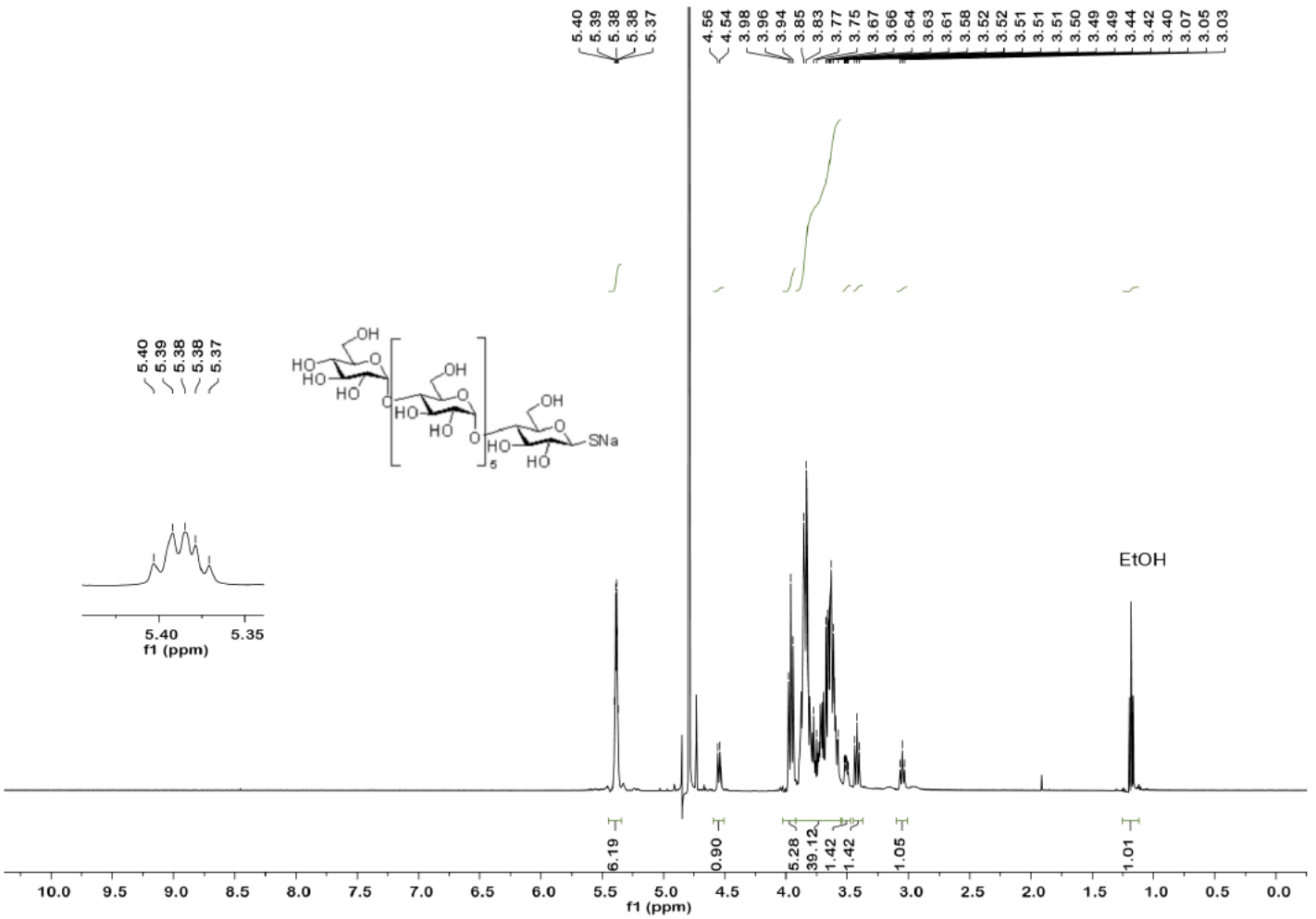

Figure S21. ^{1}H NMR spectrum of **10** in D_2O.

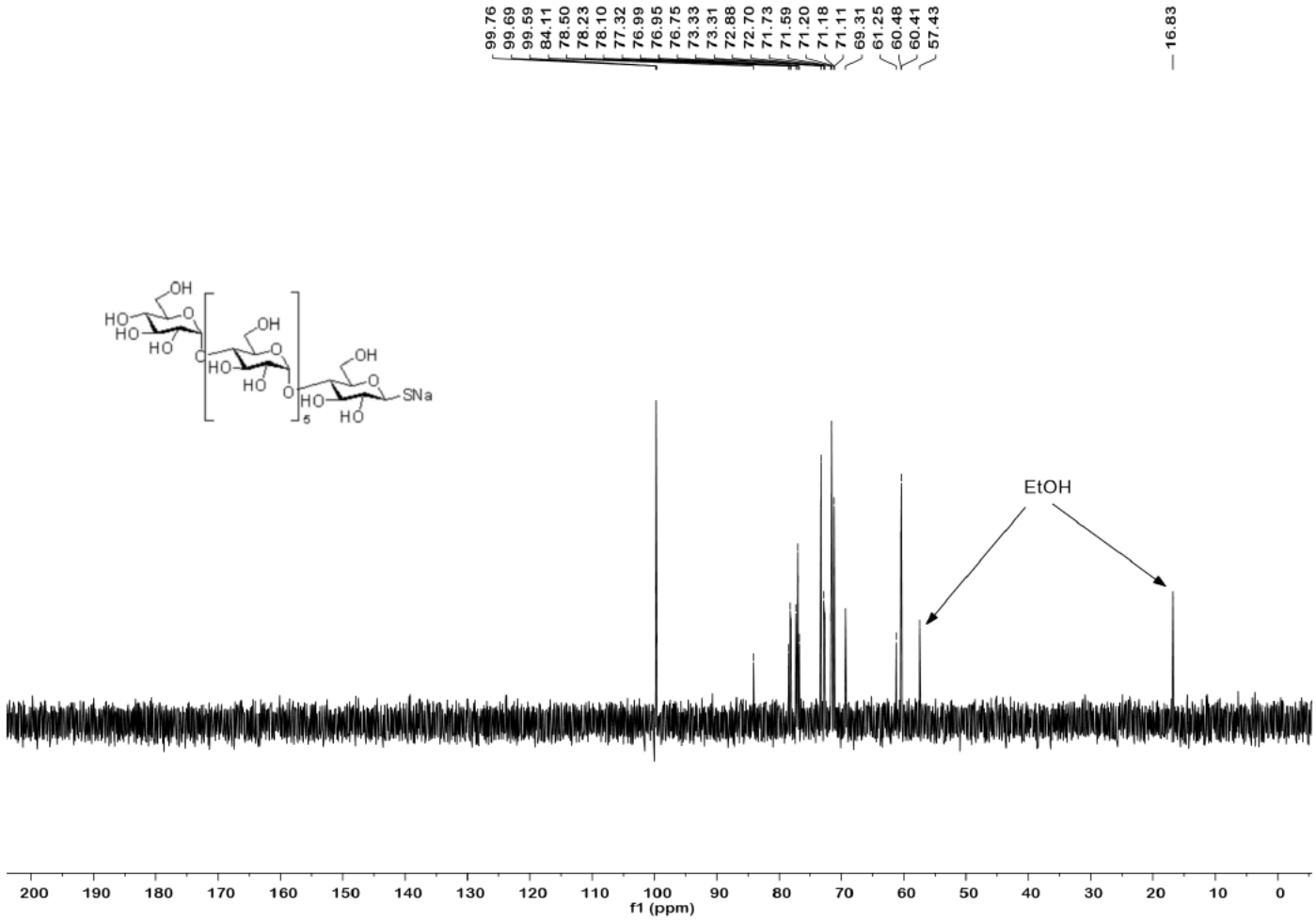

Figure S22. ^{13}C NMR spectrum of **10** in D_2O.

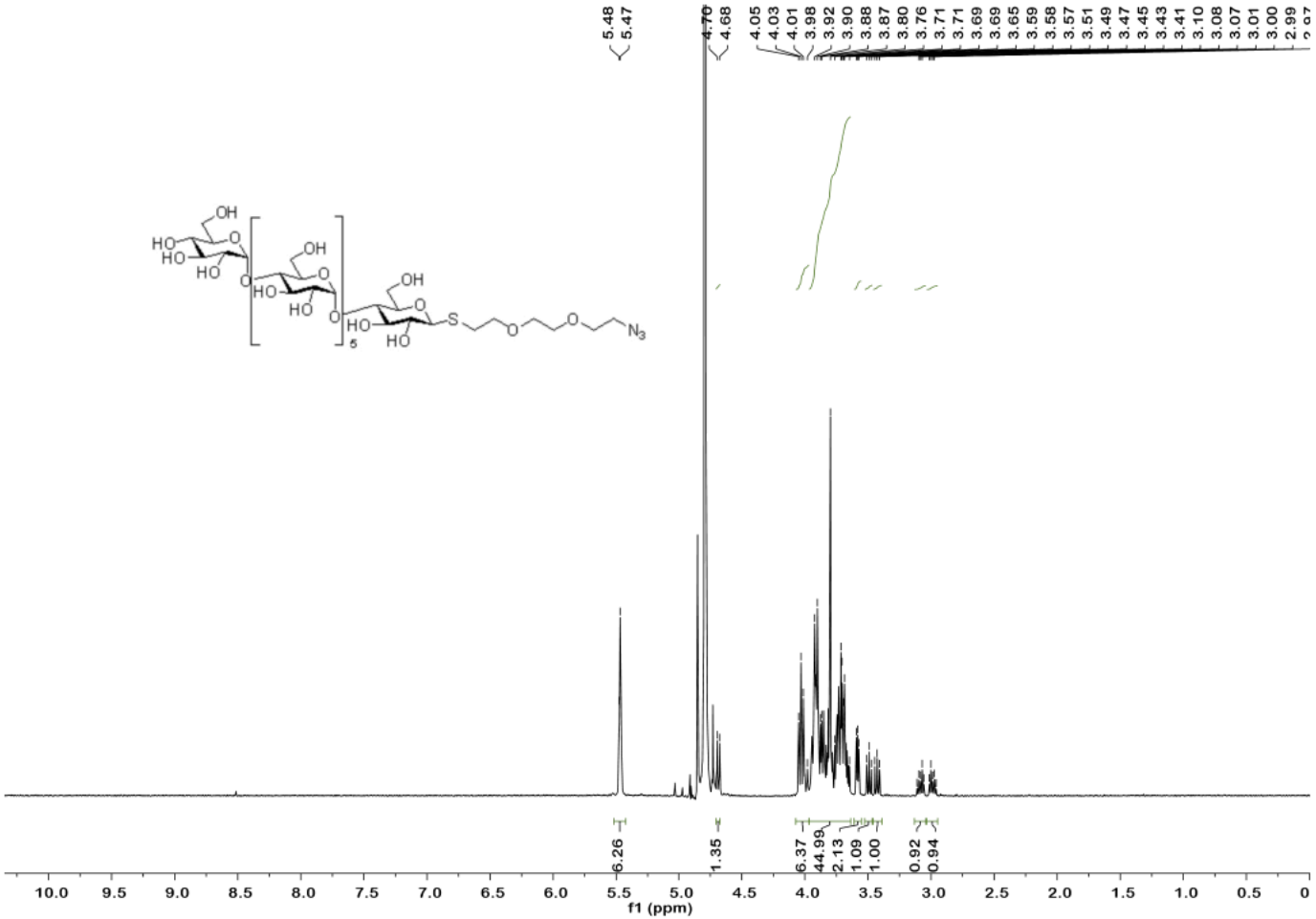

Figure S23. ^{1}H NMR spectrum of **11** in D_2O.

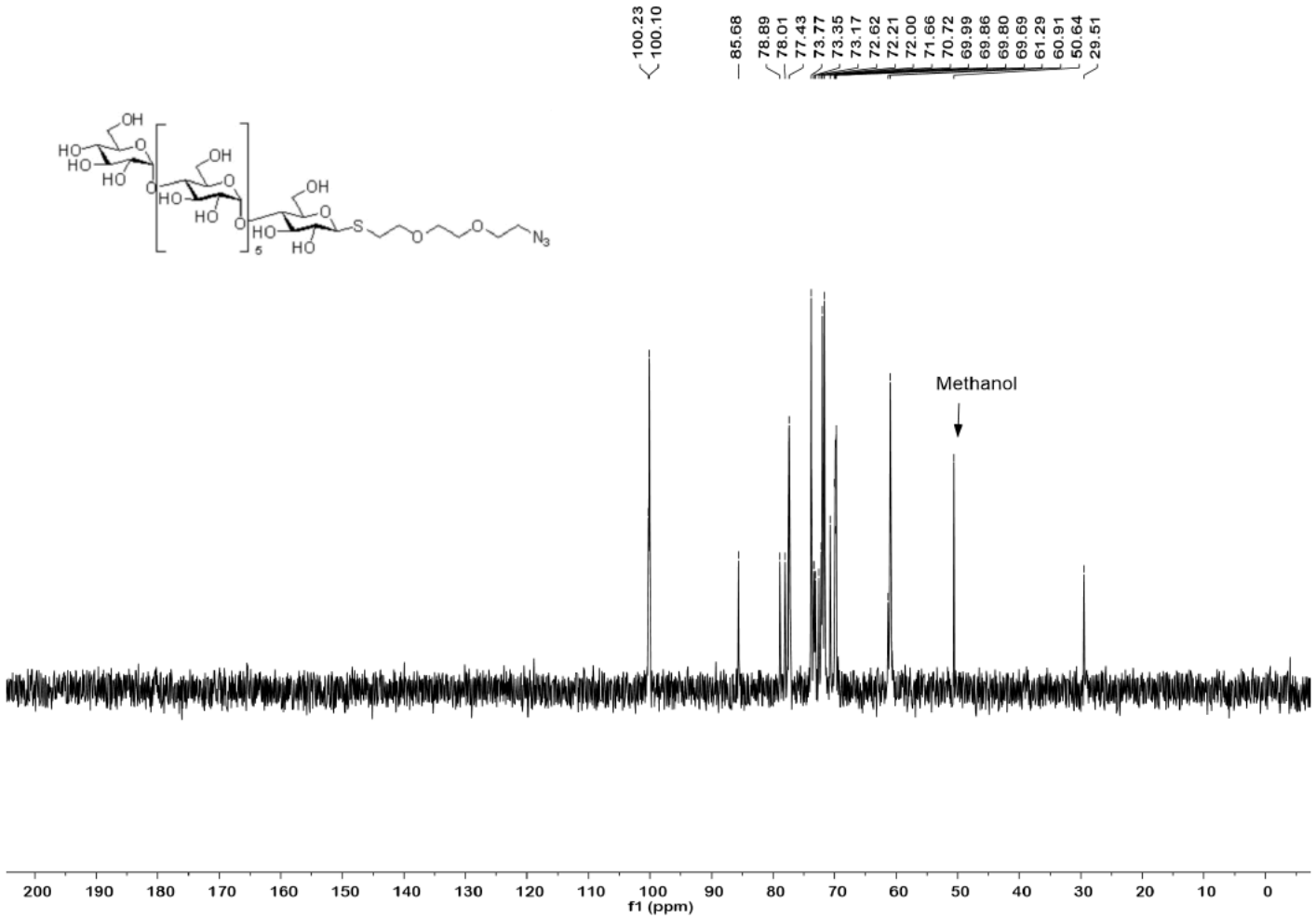

Figure S24. ^{13}C NMR spectrum of **11** in D_2O.

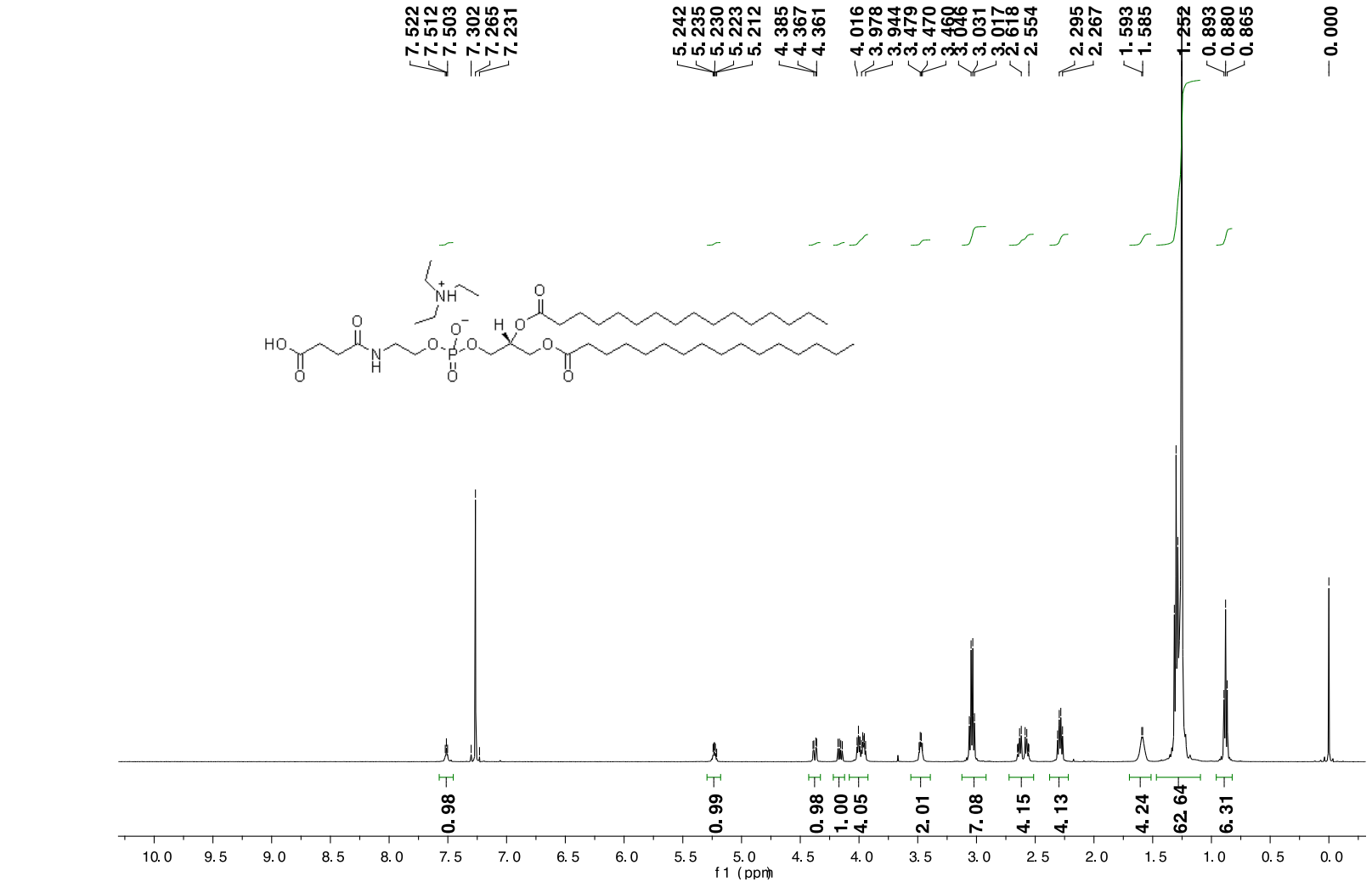

Figure S25. ^{1}H NMR spectrum of **17** in $CDCl_3$.

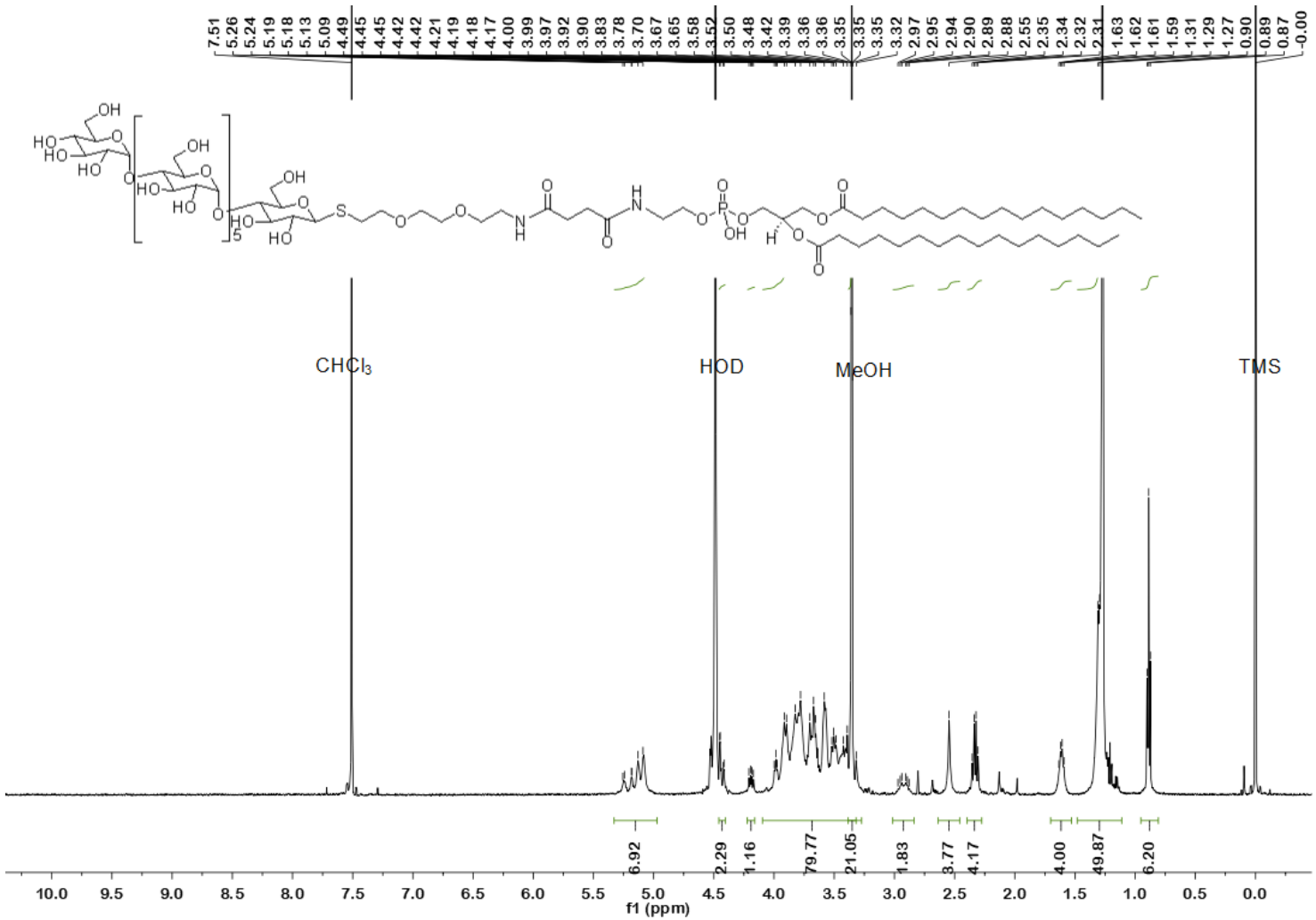

Figure S26. ^{1}H NMR spectrum of **G7-DPPE** in $CDCl_3/CD_3OD$ (7:4 v/v).

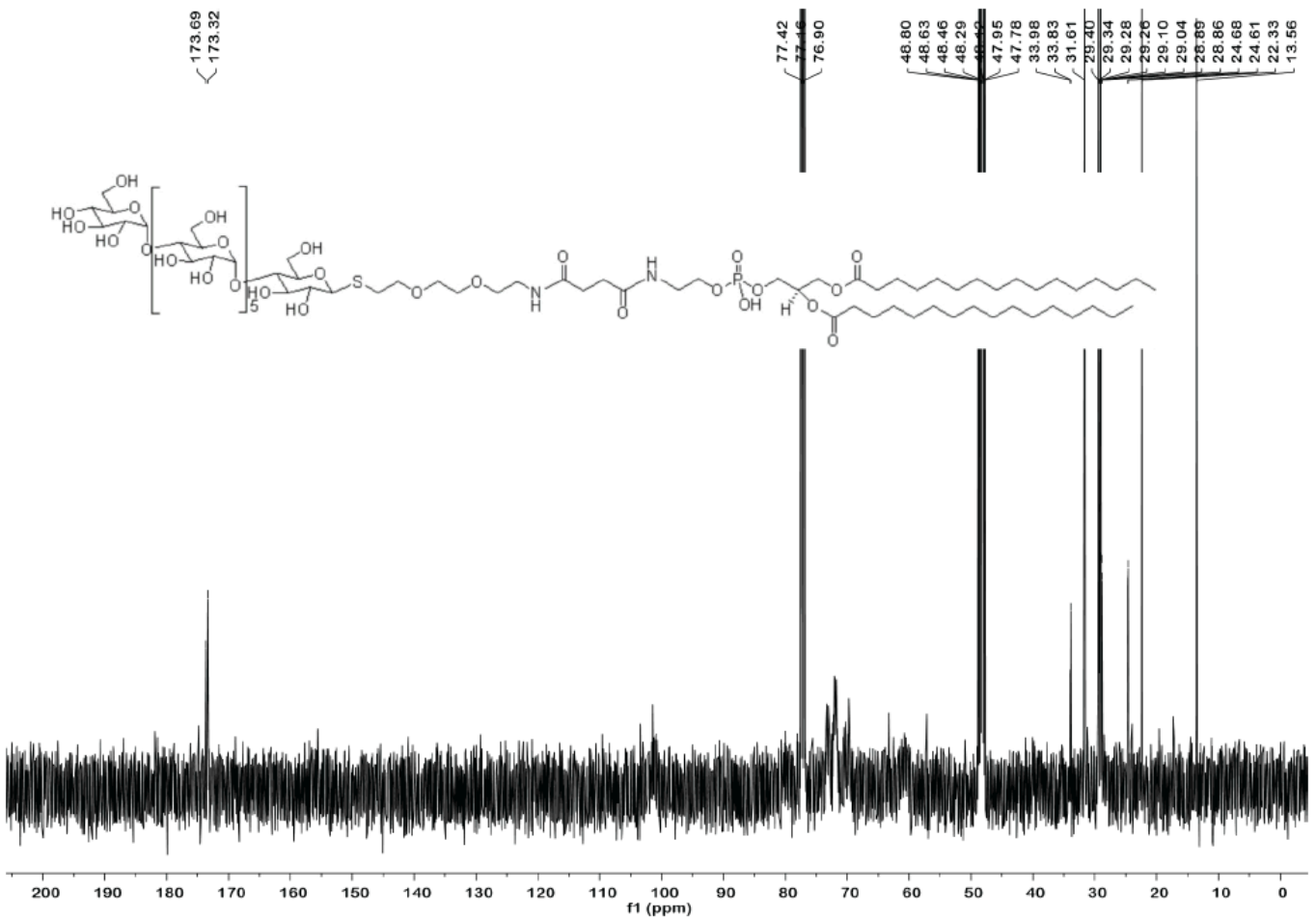

Figure S27. ^{13}C NMR spectrum of **G7-DPPE** in $CDCl_3/CD_3OD$ (7:4 v/v).

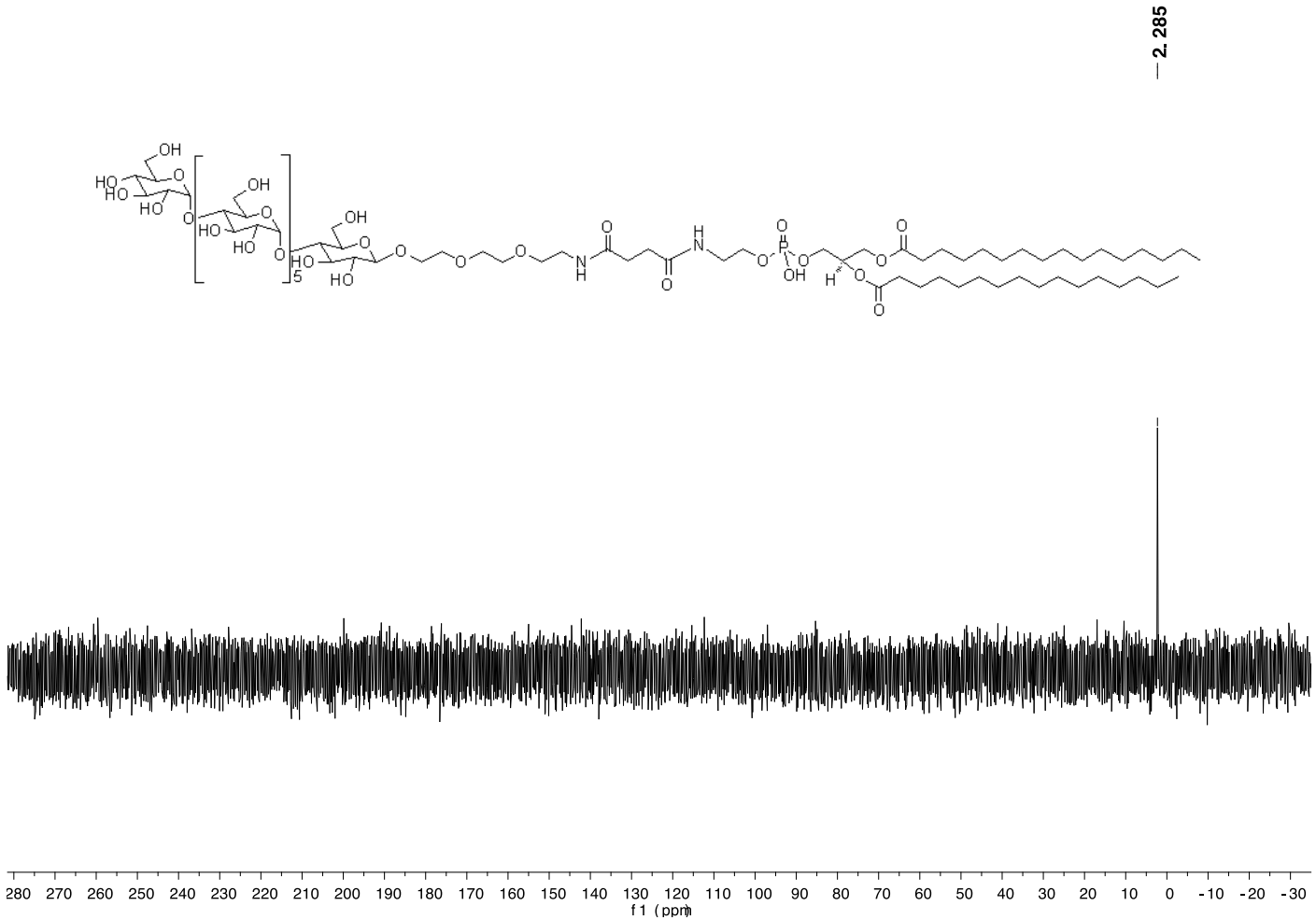

Figure S28. ^{31}P NMR spectrum of **G7-DPPE** in in $CDCl_3/CD_3OD$ (7:4 v/v).

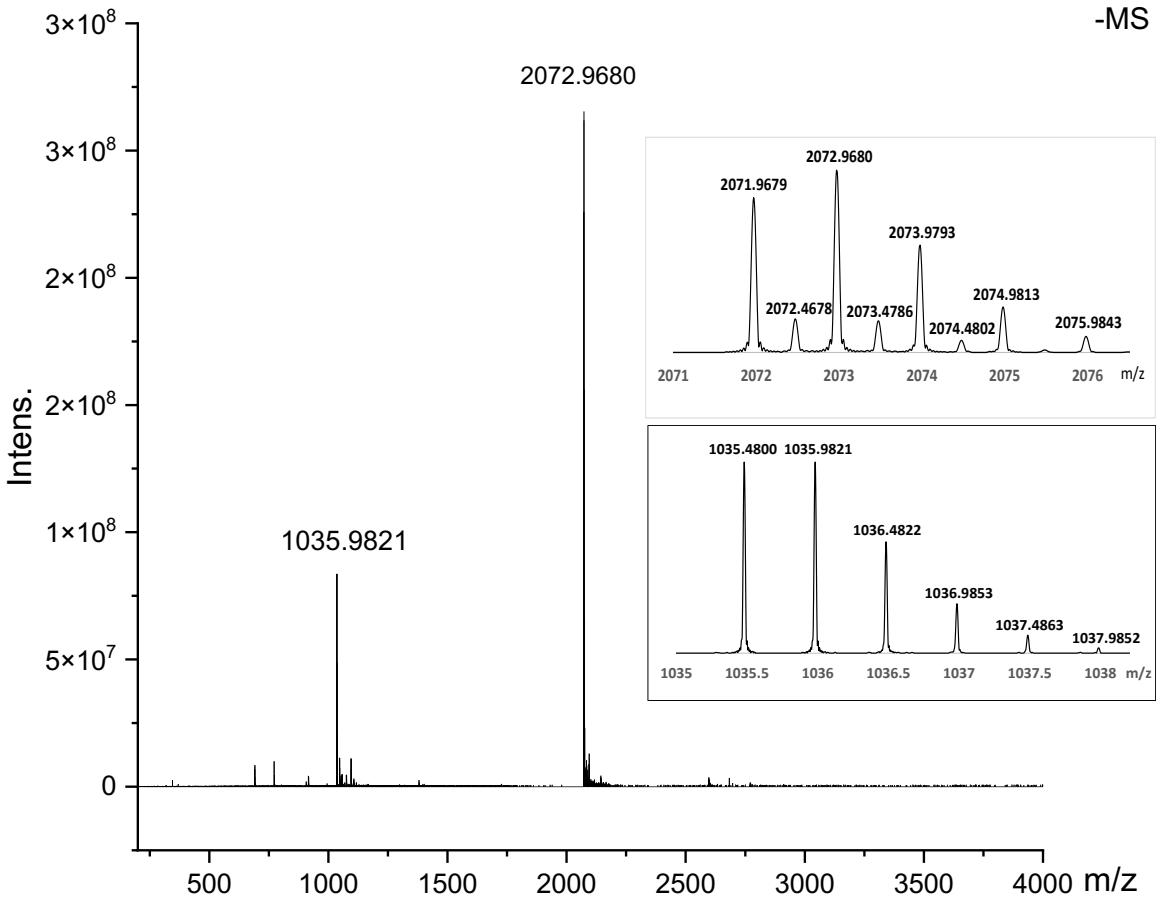

Figure S29. HRMS spectrum of **G7-DPPE.**

MS calcd. for $C_{89}H_{161}N_2O_{47}PS$ $[M\text{-}H]^-$, m/z: 2071.9655, 2072.9688, 2073.9722; $[M\text{-}2H]^{2-}$, m/z: 1035.4791, 1035.9808, 1036.4825. Found: 2071.9679, 2072.9680, 2073.9733, 1035.4800, 1035.9821, 1036.4822.

9. References

1 Norberg, O., Deng, L., Yan, M. & Ramstroem, O. Photo-Click Immobilization of Carbohydrates on Polymeric Surfaces: A Quick Method to Functionalize Surfaces for Biomolecular Recognition Studies. *Bioconjugate Chem*. **2009**, *20*, 2364-2370.

2 Deng, L., Norberg, O., Uppalapati, S., Yan, M. & Ramstroem, O. Stereoselective synthesis of light-activatable perfluorophenylazide-conjugated carbohydrates for glycoarray fabrication and evaluation of structural effects on protein binding by SPR imaging. *Org*. *Biomol*. *Chem*. **2011**, *9*, 3188-3198.

3 Schmitt, L., Dietrich, C. & Tampe, R. Synthesis and Characterization of Chelator-Lipids for Reversible Immobilization of Engineered Proteins at Self-Assembled Lipid Interfaces. *J*. *Am*. *Chem*. *Soc*. **1994**, *116*, 8485-8491.

4. Xiang, T.; Xu, Y.; Anderson, B. D., The barrier domain for solute permeation varies with lipid bilayer phase structure. *J*. *Membr*. *Biol*. **1998,** *165*, 77-90.